CHEMICAL REVIEWS

pubs.acs.org/CR Review

Deuteration for High-Resolution Detection of Protons in Protein Magic Angle Spinning (MAS) Solid-State NMR

Bernd Reif*

Cite This: https://doi.org/10.1021/acs.chemrev.1c00681 Read Online

ACCESS | Metrics & More | Article Recommendations

ABSTRACT: Proton detection developed in the last 20 years as the method of choice to study biomolecules in the solid state. In perdeuterated proteins, proton dipolar interactions are strongly attenuated, which allows yielding of high-resolution proton spectra. Perdeuteration and backsubstitution of exchangeable protons is essential if samples are rotated with MAS rotation frequencies below 60 kHz. Protonated samples can be investigated directly without spin dilution using proton detection methods in case the MAS frequency exceeds 110 kHz. This review summarizes labeling strategies and the spectroscopic methods to perform experiments that yield assignments, quantitative information on structure, and dynamics using perdeuterated samples. Techniques for solvent suppression, H/D exchange, and deuterium spectroscopy are discussed. Finally, experimental and theoretical results that allow estimation of the sensitivity of proton detected experiments as a function of the MAS frequency and the external B_0 field in a perdeuterated environment are compiled.

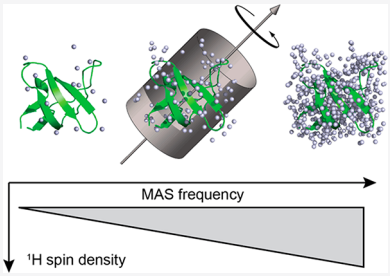

CONTENTS

1. Introduction A
2. Narrow Proton Resonances by Spin Dilution B
2.1. Amide Protons B
2.2. Methyl Protons B
2.3. Other Aliphatic Sites C
2.4. Exchangeable Side Chain Protons C
3. Solvent Suppression C
4. Paramagnetic Doping, Solvent Accessibility, and Molecular Interfaces C
5. Limits of Resolution in the Solid State D
6. Assignment Experiments D
7. Deuterium Spectroscopy E
8. H/D Exchange Experiments E
9. Quantification of Distances F
10. Quantification of Dynamics F
11. Motional Interference with Decoupling H
12. Sedimented Solutions H
13. Consequences of Deuteration on Protein Stability, Enzymatic Activity, and Function I
14. Faster MAS, Higher Fields, and Protonated Samples I
Author Information J
Corresponding Author J
Notes J
Biography J
Acknowledgments J
References J

1. INTRODUCTION

The development of magic angle spinning (MAS) solid-state NMR has made tremendous progress in the past 20 years. Improved experimental performance was triggered by the development of ever faster spinning probes.[1,2] Increased rotation frequencies result in a more efficient averaging of proton dipolar couplings, which in 2016 culminated in the determination of the first de novo protein structure which is based on proton detection by MAS solid-state NMR.[3] Initially, multipulse homonuclear decoupling sequences such as CRAMPS,[4−6] wPMLG,[7,8] and wDUMBO[9] have been employed to suppress proton homonuclear interactions in either the direct or indirect dimension. In CRAMPS type sequences, the signal is detected stroboscopically by including windows in the multiple pulse sequence. As such, the sequences are restricted to relatively low MAS rotation frequencies (<13 kHz). Windowed detection schemes come along with reduced sensitivity as large filter band widths have to be employed.

Alternatively, strong proton,proton dipolar couplings can be suppressed chemically by deuteration. There, protons are replaced with deuterons at all nonexchangeable positions. After protein expression, deuterons at exchangeable positions are replaced with protons. This approach was originally

Special Issue: Biomolecular NMR Spectroscopy

Received: August 2, 2021

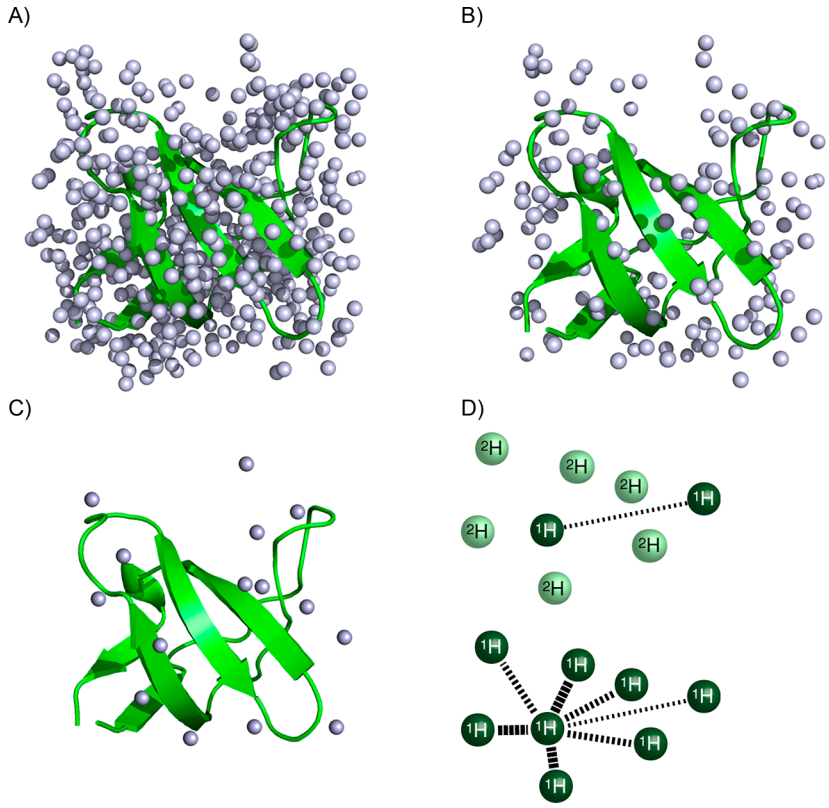

Figure 1. α-Spectrin SH3 domain at different levels of deuteration (PDB 1U06).[10] In comparison to the protonated sample (A), the number of proton dipolar interactions is already significantly reduced in the perdeuterated sample that is recrystallized from a buffer that contains 100% H_2O (B). If D_2O is admixed into the crystallization buffer, the proton spin density is further diminished (C). The attenuated proton dipolar network allows to detect protons in the solid-state with high resolution (D). Reproduced with permission from ref 11. Copyright 2012 Elsevier.

introduced for solution NMR.[12−14] In the solid state, deuteration was first employed to study small molecules,[15−17] then later extended to the investigation of peptides[18−20] and proteins.[21−24] Deuterons have a 6.5-fold smaller magnetogyric ratio compared to protons. This facilitates homonuclear and heteronuclear decoupling. The dilution of the proton spin system by deuteration is illustrated in Figure 1.

2. NARROW PROTON RESONANCES BY SPIN DILUTION

2.1. Amide Protons

Spin dilution at exchangeable sites yields high resolution amide proton proton spectra in perdeuterated proteins at MAS rotation frequencies on the order of 10−20 kHz.[25] The experimental proton line widths are on the order of 17−35 Hz, which is equivalent to 0.028−0.058 ppm at 600 MHz. Early examples and applications of this labeling strategy involve the investigation of the membrane protein DsbB reconstituted in a lipid environment.[26] In this work, the resonances of DsbB were assigned using ^{1}H-detected 3D NMR experiments. Lakomek et al. investigated and compared solid- and solution-state lipid nanodisc preparations in which the outer-membrane protein OmpX was reconstituted.[27] Furthermore, proton detection experiments have been employed to probe the PET ligand binding site in Alzheimer's disease Aβ40 fibril.[28] For hepatitis B virus capsids, it has been shown that back-substitution of exchangeable deuterons with amide protons improves the proton resolution at 100 kHz MAS by a factor of 1.5 in comparison to a protonated sample.[29] The average proton line width decreases from 170 to 110 Hz, which corresponds to a decreased from 0.20 to 0.13 ppm at 850 MHz. However, because of solvent inaccessibility, 15% of all amides are absent in the spectra of the deuterated protein because exchangeable protons cannot easily be back-substituted in the reconstitution process.

2.2. Methyl Protons

Similarly, methyl protons can be observed at high resolution in perdeuterated peptides and proteins.[30] The media that are employed to grow bacteria and overproduce the protein of interest contain glucose that is labeled only with an efficiency of ∼97−98% with deuterium. Thus, there is a 6−9% probability to find a proton in a methyl group. At 600 MHz (14.1 T) and using a MAS rotation frequency of 22 kHz, an experimental proton (carbon) line width of 20−25 Hz (5−8 Hz) was observed. Use of specific amino acid precursors such as pyruvate[31] and α-ketoisovalerate[32−34] during protein biosynthesis allows selectively labeling of methyl groups and increasing of the sensitivity further. For liquid-state NMR, this labeling strategy was pioneered by Kay and co-workers.[35] Even higher performance is obtained by making use of stereospecific precursors which yield enrichment in only one of the two pro-chiral methyl groups in valine, leucine, or isoleucine[36] as well as for methionine, threonine, and alanine.[37] In the solid state, the intramethyl proton dipolar couplings can potentially impact resolution. Therefore, CHD_2 isotopomers should be incorporated into the protein.[38] In addition, care has to be taken to decouple deuterium scalar couplings while evolving carbon chemical shifts. The ^{2}H,^{13}C scalar coupling is on the order of 20 Hz. As deuterium is a spin-1 nucleus, scalar couplings contribute significantly to the achievable ^{13}C line width.

https://doi.org/10.1021/acs.chemrev.1c00681
Chem. Rev. XXXX, XXX, XXX−XXX

2.3. Other Aliphatic Sites

Randomly protonated (RAP) samples are obtained by growing bacteria in a medium containing $^{2}H,^{13}C$ labeled glucose in the presence of varying amounts of H_2O (5−20%).[39] Using this procedure, samples are obtained that are randomly protonated in the side chain.

A M9 medium that is supplemented with 5% [15%] H_2O yields approximately 7% [17%] protons in the Cα position. Under these conditions, a labeling efficiency of 3% [14%] and 1% [12%], respectively, is observed for methylene and methyl groups. Side chain resonances are assigned in HCCH type experiments in a straightforward manner.[40,41] If faster MAS frequencies are available, larger amounts of H_2O in the M9 medium are tolerable. In addition to line broadening that is induced by proton−proton dipolar couplings within the methyl group, mixtures of isotopomers result in an apparent broadening of the resonances and in a deterioration of the spectral resolution.

An admixture of 15 and 25% H_2O into the M9 medium yields high sensitivity and resolution in the MAS frequency regime of 50 kHz. For these kinds of samples, an average ^{1}H line width of 40−50 Hz is observed.[42] $^{1}H,^{13}C$ correlation spectra of RAP samples yield almost comparable intensities in comparison to samples in which α-ketoisovalerate was used as a precursor.[43] RAP labeled samples are readily prepared and allow obtaining of methyl spectra from all methyl containing amino acids without the need to use specific amino acid precursors.[36] The RAP labeling scheme has been successfully applied to a fibril sample of the HET-s (218−289) prion protein.[44] An approach coined inverse fractional deuteration employs protonated glucose and D_2O to achieve a similar effect.[45,46] Alternatively, protonated amino acids are added to the growth medium that consists of deuterated glucose and D_2O to selectively introduce protons into protein.[47] Use of transamination enzymes allows to yield quantitative protonation at the backbone Hα position.[48] In the approach, the keto acid is transformed by transaminases into the respective amino acid. The proton that is bound to the Cα carbon originates from the solvent. Racemization is avoided because the correct L-amino acids are generated enzymatically.

2.4. Exchangeable Side Chain Protons

Hydroxyl protons exchange rapidly with the solvent. Due the fact that they experience only weak couplings with their environment, hydroxyl protons are difficult to assign in solution NMR. By making use of dipolar couplings, magnetization can be transferred approximately 50× faster in the solid state. In a long-range $^{1}H,^{13}C$ cross-polarization experiment, all threonine hydroxyl protons could be assigned in the α-spectrin SH3 domain by correlating the OH proton and the Cα/Cβ resonances.[49] An additional delay during which magnetization is stored longitudinally yields the exchange properties of the respective hydroxyl protons. Similarly, collective exchange processes in the active-site proton cage in bacteriorhodopsin could be characterized.[50] Furthermore, backbone hydrogen bonds that stabilize protein secondary structure elements in solid proteins could be identified.[51] The same experiment applied to side chain resonances showed that salt bridges stabilize amyloid quarternary structure.[52] By using a similar strategy, the hydrogen bonding topology of histidines in the influenza M2 channel has been identified.[34] More recently, the hydrogen bonding topology could be characterized by quantifying the scalar coupling across a hydrogen bond.[53] These experiments are carried out with a protonated sample that is rotated with a frequency of 100 kHz.

3. SOLVENT SUPPRESSION

Biological solid-state samples contain a fair amount of aqueous buffer to keep samples hydrated. In ^{1}H detected experiments, water suppression thus becomes an issue. It was shown that pulsed field gradients can be employed to attenuate the water resonance.[21] Alternatively, a constant-time-like indirect evolution period in combination with proton decoupling allows efficient cancellation of unwanted solvent magnetization.[24] The MISSISSIPPI sequence[54] combines these two approaches and is nowadays the most widespread employed pulse sequence element to achieve efficient water suppression. Gradients are not essential for the MISSISSIPPI sequence but improve water suppression significantly. Care has to be taken to avoid an attenuation of the resonances of the protein by a transfer of saturation from the water pool. Therefore, water suppression should be combined with water flip-back pulse schemes which return the water magnetization back along the z-axis prior to detection.[55] Water flip-back pulses facilitate spin recovery and enable faster recycle delays. At the same time, a potential saturation transfer from water to the protein resonances is avoided.

4. PARAMAGNETIC DOPING, SOLVENT ACCESSIBILITY, AND MOLECULAR INTERFACES

Sensitivity can be improved by reducing the recycle delay of the experiment making use of complexed paramagnetic ions, such as, e.g., Cu-EDTA.[56−58] This way, the recycle delay in the experiment can be decreased by up to 15-fold. At the same time, the proton line shape is largely unaffected. Perdeuterated samples do not require high-power proton decoupling. Thus, long acquisition times and short recycle delays on the order of 0.3 s are possible without compromising the sample quality. The paramagnetic relaxation agent in solution can be employed to furthermore access solvent-PREs. Solvent-PREs were originally introduced in solution NMR to aid the protein structure determination process[59] and were exploited in the solid state to characterize protein−protein interfaces.[60] The solvent accessible surface can be characterized by quantification of the difference ^{1}H-T_1 relaxation rate that is obtained for samples with and without complexed paramagnetic ions.[61] Alternatively, molecular interfaces can be probed by comparing the spectra of a perdeuterated, ^{15}N labeled protein in the presence of a deuterated versus a protonated ligand. The differential broadening of amide resonances due to dipolar interactions with the ligand were exploited to identify the interface between a box C/D RNA and the binding L7Ae protein.[62] Similarly, the ligand binding interface can be determined by making use of magnetization transfer from a protonated ligand to the carbon resonances of a perdeuterated protein, as shown for Congo Red interacting with HET-s(218−289) prion fibrils.[63] Similarly, the interface between CAP-Gly and microtubules could be determined. This was achieved by making use of dREDOR filtered experiments.[64]

In case the concentration of protons at exchangeable sites cannot be adjusted prior to the NMR experiment by refolding the protein in an appropriate buffer, perdeuteration can be an issue because certain amides in structured regions might be strongly protected from exchange. Back-exchange of deuterons with protons then becomes impossible. On the other hand, the

https://doi.org/10.1021/acs.chemrev.1c00681
Chem. Rev. XXXX, XXX, XXX−XXX

absence of certain amide resonances allows identification of the solvent-exposed parts of the protein, as has been shown for the seven-helical integral membrane proton pump proteorhodopsin.[65] In addition to residues located at the membrane interface, residues are also observed that are located in helix G, suggesting that the F−G loop may have a high mobility and transiently expose a hydrophilic cavity in the extracellular half of the protein which might be part of a proton-conducting pathway. Similarly, the spectra of fully protonated and perdeuterated proteorhodopsin were compared to yield the assignment of the nonsolvent accessible core of the protein.[66]

Direct interactions between the solvent and the human voltage dependent anion channel, and the alkane transporter AlkL, respectively, are probed by recording a 3D HhNH correlation spectrum in which proton−proton mixing is achieved via spin diffusion.[67] Similar experiments were carried out for the potassium channel NaK2K.[68] It was shown that the conduction pathway of the potassium channel is free of water under physiological conditions. Lange and co-workers have furthermore investigated the structure and dynamics of the rhomboid protease GlpG reconstituted in liposomes and have confirmed the presence of water molecules in the catalytic cavity.[69] Dynamics measurements revealed a dynamic hotspot of GlpG that is important for gating. Alternatively, the binding interface can be probed by analyzing the differential dynamics in the presence and absence of a ligand. This has been shown for protein G in complex with a full-length human immunoglobulin.[70,71] In addition to chemical shift perturbations, R_1 and $R_{1\rho}$ relaxations rates suggest an increased amount of slow motions with a time scale in the >500 ns range in the complex.

In a very favorable case, a proton detected experiment allowed to detect a structured water molecule in the conductance domain of the homotetrameric influenza A M2 membrane protein.[72] The bound water molecule was observed at a proton chemical shift of 11 ppm and was found to be hydrogen bonded to H37-δ1 in the channel.

5. LIMITS OF RESOLUTION IN THE SOLID STATE

In the solid state, the NMR line width is dependent on several factors. Inhomogeneous broadening[73] results in a distribution of chemical shifts, for example, in a sample which is structurally heterogeneous. By contrast, homogeneous broadening is a consequence of dynamics and thus relaxation. In the following, the factors that affect resolution at the upper limit where sample heterogeneity is not an issue shall be discussed.

The decoupling performance and the accuracy of the magic angle have a major impact on the resonance line width in solid-state NMR. For perdeuterated samples, however, the decoupling performance is not compromising the spectral quality because long acquisition times can be employed without damaging the sample. Mis-adjustments of the sample rotation angle results in a broadening of the resonance.[74,75] The spinning angle can be optimized by monitoring the H−N *J*-coupling spin echo signal in the protein sample under investigation.[76] Spin-state selective experiments that select a particular multiplet component, for which the ^{1}H−^{15}N dipole−dipole interaction and the ^{15}N CSA mutually cancel each other at high field due to interference of anisotropic interactions allow furthermore to overcome magic angle mis-settings.[77] The quality of the shim is another factor that potentially contributes to line broadening. However, the residual proton line width of the water resonance is less than 1 Hz in a typical microcrystalline protein sample, suggesting that the homogeneity of the magnetic field does not limit the resolution of the ^{1}H detected experiments. On the other hand, the proton dipolar network directly impacts the resolution in a ^{1}H detected experiment. At a certain degree of deuteration and MAS frequency, however, the spectral quality cannot be improved further,[25,78−81] suggesting that proton dipolar interactions are not the critical factor that determines the resolution of the proton spectrum. Protein dynamics and thus incoherent effects have a further influence on the proton line width. The experimental relaxation data can be employed to calculate the resonance line width that results from dynamics.[82] It is found, however, that dynamics contributes less than 2 Hz to line width for most residues in the α-spectrin SH3 domain.

Another factor that potentially affects line width is the anisotropic bulk magnetic susceptibility (ABMS).[1,83] In a powder sample, the individual crystallites are nonhomogeneously distributed. Crystallites and mother liquor have a distinct bulk magnetic susceptibility (BMS). The induced magnetic polarization from the external magnetic field produces a screening field that results in an inhomogeneously broadened resonance line. The crystallites appear as magnetic dipoles in the liquid. If the microcrystallites would be spherical, the BMS would be isotropic and could be fully spun out by MAS. However, given the fact that microcrystals, fibrils, or lipid reconstituted membrane proteins are not spherical, the strength of the induced dipolar fields depends on their orientation with respect to the external magnetic field. The ABMS Hamiltonian has a similar dependence on the nuclear spin part as the isotropic chemical shift.[1] Application of a Carr−Purcell−Meiboom−Gill (CPMG) train of pulses yields a significantly extended coherence lifetime.[84−86] A significantly extended FID is obtained if CPMG pulses are applied in either the indirect or direct evolution period in a ^{1}H,^{15}N correlation experiment.[87] This suggests that ABMS is responsible for the finite line width in the solid-state.

6. ASSIGNMENT EXPERIMENTS

Assignments of perdeuterated and back-exchanged proteins in rotating solids is nowadays routinely achieved using the suite of experiments suggested by Barbet-Massin et al.[88] These experiments are employed as well now for fully protonated samples at >110 kHz MAS.[3,89] Alternative strategies are suggested by Lange,[90] Meier,[91] and co-workers.

Coherences in the solid state are long-lived enough to enable *J*-coupling based assignment experiments for perdeuterated samples such as 3D HNCA, HNCO, and HNCACB.[92,93] Penzel et al. have compared scalar and dipolar coupling based transfer sequences.[91] Even scalar couplings across hydrogen bonds in proteins can be quantified reliably.[53,94] This experiment is intrinsically very insensitive due to the necessary long de- and refocusing delays. In contrast to solution NMR, however, the achievable resolution and line width in the solid state are not determined by nuclear relaxation implied by molecular tumbling. Therefore, small scalar couplings are in principle accessible in the solid state.

Barbet-Massin and co-worker mostly employ scalar transfer elements to mediate homonuclear magnetization transfer. Alternatively, band-selective homonuclear cross-polarization (BSH-CP) can be employed to yield transfer of magnetization between the carbonyl and Cα carbon atoms.[95,96] The experiment works well for high magnetic fields and MAS frequencies on the order of 20 kHz. Under these conditions, the ^{13}CO,^{13}Cα isotropic chemical shift difference is greater than the MAS frequency. Recoupling is obtained when the sum of the effective

https://doi.org/10.1021/acs.chemrev.1c00681
Chem. Rev. XXXX, XXX, XXX−XXX

rf fields [$\omega_1^{eff}(^{13}CO) + \omega_1^{eff}(^{13}C\alpha)$] matches 2× ω_R. This method can directly be employed in assignment experiments such as a 3D-(H)CO(CA)NH experiments to obtain inter-residual connectivities in the protein backbone. The assignment process can be supplemented with amide−amide connectivities obtained from (H)N(CACO)NH or (H)N(COCA)NH type 3D[97,98] and 4D[99] experiments. The resulting connectivities are diagonal-free and can be employed for automatic backbone assignment, e.g., in UNIO-MATCH.[100,101]

Combination of direct ^{13}C Boltzmann polarization and magnetization transferred from directly bonded or remote protons can increase the sensitivity of the experiment.[102,103] Carbon mixing over multiple bonds using TOBSY[104] or MOCCA[105] sequences enables access to virtually all side chain carbon chemical shifts and can be detected either on the methyl[30] or amide proton.[102,106]

To speed up the sampling process, GFT and APSY have been introduced to biological solid-state NMR. GFT projection experiments are based on synchronous evolution of multiple nuclei in a single dimension. The convoluted spectra are added and subtracted to yield the reconstructed pure chemical shift spectra. GFT projection experiments have been recorded from 4D/3D (HA)CANCOCX and 3D/2D (HACA)NCOCX experiments.[107] Automated projection spectroscopy (APSY) was originally introduced by Hiller and Wüthrich for solution NMR[108,109] and recently applied in the solid state.[110,111] The 5D peak lists that are reconstructed from a number of 2D projections of a 5D-(H)NCOCANH experiment are a next step toward an automated assignment of the protein backbone.[111] The efficiency of the pulse scheme is ensured by long $T_{1\rho}$ and T_2' coherence lifetimes in the solid state. Additionally, pairs of 4D experiments that correlate HN_i/N_i with CA_i/CO_i or CA_{i-1}/CO_{i-1} allow to obtain sequential connections with high confidence.[112,113]

7. DEUTERIUM SPECTROSCOPY

In the perdeuteration approach described here, deuterons are primarily introduced into the sample to attenuate the ^1H dipolar network to achieve proton line narrowing. On the other hand, deuteron can be employed actively for spectroscopy in the solid state. Given the fact that overall tumbling is absent in immobilized systems, high-resolution $^2H,^{13}C$ correlation experiments can be obtained.[75,114] ^2H double quantum (DQ) coherences yield an improved spectral resolution.[115] Sensitivity is not compromised by missetting of the rotation axis from the magic angle. At the same time, coherences are less sensitive to dynamics that potentially interferes with refocusing of the anisotropic interaction by MAS. DQ spectroscopy effectively doubles the spectral resolution because ^2H DQ coherences precess 2-fold faster in comparison to single quantum (SQ) coherences.[75]

Deuterium is the paradigmatic nucleus to study molecular motion in solids.[116,117] Deuterium has been employed in the past to investigate synthetic polymer,[118] lipid,[119,120] and protein dynamics[121,122] of static samples. Using small increments in the indirect evolution period allows reintroduction of the deuterium Pake pattern under slow MAS and to retrieve dynamic information.[123−127] $^2H,^2H$ spin diffusion potentially compromises the deuterium spinning sideband pattern in $^2H,^{13}C$ correlation experiments and the extracted anisotropy parameters.[128,129] Similarly, deuterium spectroscopy has been used to study the dynamic properties of carbohydrates and bacterial cellulose.[130]

The ^2H RF field strength determines the $^2H,^{13}C$ magnetization transfer efficiency and should exceed >80 kHz for a rigid deuteron. This power can so far only be achieved in MAS probes that operate in double channel mode. Use of optimal control (OC) derived pulse sequences allows this problem to be partially overcome.[131] Promising results were obtained with the RESPIRATION scheme, where rf amplitudes were restricted to a maximum of 50 kHz (with an average rf field of 11 kHz). However, more work is needed to design pulse sequences that use even lower rf fields and are able to access backbone Cα or other methine chemical groups. To fully exploit the potential of deuterium in multidimension correlation experiments, a four-channel MAS solid-state NMR probe is needed that is equipped with a high power deuterium channel and a sensitive magic angle adjustment, so that deuterium spectroscopy and proton detection can be concatenated and combined with amide correlation experiments.[132]

Deuterons can serve as magnetization entry point for any multidimensional NMR experiment. Combination of direct ^{13}C Boltzmann polarization and magnetization transferred from directly bonded or remote deuterons can increase the sensitivity of the experiment.[133]

8. H/D EXCHANGE EXPERIMENTS

Different H/D exchange experiments that make use of perdeuterated samples have been suggested recently. Lopez del Amo et al.[134] propose an experiment which makes use of the deuterium isotope effect on the amide nitrogen chemical shift for perdeuterated protein samples that are recrystallized in a buffer that contains a significant amount of D_2O. Exchange is probed by direct ^{15}N detection or by concatenating two exchange mixing times in combination with proton detection and $^{15}N-^1H/^{15}N-^2H$ isotope filtering elements. The experiment is sensitive to H/D exchange times of up to 30 s, which reflects the typical amide nitrogen relaxation time in a protein. Deuterium back-exchange experiments at labile sites were carried out for a perdeuterated, fully proton back-exchanged *Escherichia coli* type I pili sample to investigate solvent accessibility.[135] For that purpose, a preassembled reprotonated pili sample was washed several times with nondenaturing 100% D_2O buffer to remove all solvent accessible labile protons. It was found that amide protons protected from H/D exchange are mostly found in the core of the monomeric subunits of the pili, while high H/D exchange rates are observed in lateral and axial intermolecular interfaces. The HDX data thus allows to get a better understanding of the stability and mechanical properties of the pili.

Hydrogen exchange affects the ^{15}N longitudinal relaxation time of amides in a protein. Comparison of ^{15}N-R_1 values measured for samples that are prepared with different amounts of D_2O in the buffer allows quantification of the exchange rate. This approach is coined Relax-EXSY and was employed to determine amino acid specific exchange rates in the type III secretion system needle protein.[136,137] The experiments described above are equilibrium experiments. By contrast, Grohe and co-worker have suggested a nonequilibrium experiment to probe backbone amide hydrogen−deuterium exchange rates in the solid state.[138] In the experiment, the supernatant buffer of a 100% back-substituted microcrystalline protein sample was replaced with a 80% deuterated buffer before the sample was packed the into a 1.3 mm MAS rotor. Peak intensities were monitored for 2 weeks to identify H/D exchange in real time.

https://doi.org/10.1021/acs.chemrev.1c00681
Chem. Rev. XXXX, XXX, XXX−XXX

9. QUANTIFICATION OF DISTANCES

In the presence of strong dipolar couplings, the evolution of weak interactions is attenuated. This effect is referred to a dipolar truncation.[139,140] As a consequence, it is difficult to obtain long-range distance information in uniformly isotopically labeled samples. In carbon-detected experiments using protonated protein samples, dipolar truncation effects are avoided by preparing carbon spin dilute samples. These samples can be obtained by overexpressing proteins using a medium that contains, e.g., either [1,3]-^{13}C-glycerol or [2]-^{13}C-glycerol as the only source for carbon atoms.[141,142] In fully isotopically labeled samples, third-spin assisted recoupling mechanism can potentially facilitate homonuclear long-range magnetization transfer via the proton spin reservoir. This effect is exploited in PAR[143−145] and PAIN[146,147] experiments. In perdeuterated proteins, the proton spin bath is naturally dilute. Only exchangeable sites are protonated. This labeling scheme thus facilitates the quantification of long-range proton distance restraints.[18,22,23] C7[148] derived ^{1}H,^{1}H dipolar recoupling experiments work well for microcrystalline peptides[18] but are not very efficient for microcrystalline protein samples,[22] presumably due to the presence of tightly bound water molecules which perturb the idealized 2-spin system. Spin diffusion,[149] RFDR,[150] or DREAM,[151] like mixing sequences, however, are suitable to recouple proton−proton dipolar interactions at least at moderate rotation frequencies.[22,33,152−154] Even though proton RFDR and DREAM have been successfully used at 100 kHz MAS,[89,155] novel recoupling schemes will be needed to increase the efficiency of the magnetization transfer at even faster MAS frequencies.[156]

In addition, selective labeling of methyl groups yields proton spin dilution and access to methyl−methyl and methyl−amide distance restraints.[152,154,157,158]

For methyls, care has to be taken to label samples with CHD_2 isotopomers in case experiments are carried out with MAS rotation frequencies below 50 kHz because dipolar interactions are otherwise not sufficiently removed by MAS.[159] RAP labeling yields randomly protonated samples, and this way allows to obtain distance retraints for other aliphatic sites.[39] Beyond methyls, selective labeling of amino acids is possible via the SAIL approach.[160,161]

Using proton−proton distance restraints, the structure of the dimeric (2 × 16 kDa) Zn(II)-loaded superoxide dismutase could be determined by solid-state NMR experiments.[162] In these experiments, RFDR[163] is employed to recouple proton spins.

The NMR structure of an influenza A M2 variant, S31N, that confers drug resistance, was obtained using selectively methyl protonated protein samples.[34] There, methyl−methyl distance restraints were obtained from a 4D proton detected ^{1}H−^{1}H RFDR experiment. The experimental setup is similar to an earlier implementation in which DREAM has been used for proton−proton mixing.[33] Proton chemical shift information from histidine side chains allowed to conclude further on the mechanism of H+ transport which is critical for viral replication. 3D (H)NHH and (H)N(HH)NH correlation spectra of a deuterated OmpG sample in which the exchangeable sites contained protons close to 100% allowed to identify amide−amide through-space connectivities and to determine the β-sheet topology in the β-barrel membrane protein.[164]

Exact eRFDR distance restraints are obtained in 3D ^{15}N-edited RFDR spectra (H-RFDR-hNH) experiments.[165] Quantification of the magnetization buildup in the initial-rate regime in combination with a spin-diffusion correction is required to yield exact distances. The exact distance restraints facilitate the convergence of the structure calculation process and result in a better defined structure.

Long-range distance restraints (up to ∼2 nm) can be obtained furthermore by measuring PREs. For superoxide dismutase, PRE restraints were obtained from ^{15}N-R_1 relaxation difference rates measured using a Cu^{2+}, Zn^{2+}, and a Cu^{+},Zn^{2+} complexed protein sample.[153] In combination with ^{1}H,^{1}H distance restraints, PRE restraints were shown to be extremely valuable to determine the structure of the protein in the solid state. Furthermore, pseudocontact shifts can be employed as well in the solid state to aid the structure determination process for metalloproteins.[166,167]

In case no natural metal binding sites are available, the protein under investigation, paramagnetic centers can be engineered into a protein side chain using, e.g., a suitable Cu(II)-affinity tag.[168] Backbone amide ^{15}N longitudinal and ^{1}H transverse relaxation rates for the paramagnetic and diamagnetic samples are quantified in proton-detected experiments to determine distances between the paramagnetic center and the respective amide sites in the protein. The sparse PRE restraints allow calculation of highly accurate protein structures.[169,170]

Using Gd^{3+} paramagnetic ions bound to molecular cages chelated to the lipid headgroups, it was possible to determine the orientation of the D1 domain of the membrane-associated nonstructural protein 5A (NS5A) of hepatitis C virus with respect to the lipid membrane.[171]

10. QUANTIFICATION OF DYNAMICS

NMR experiments allow obtaining access to quantitative motional amplitudes and rates. Different solid-state NMR experiments are sensitive to dynamics occurring on different time scales: relaxation experiments yield information on fast to intermediate time scale (ps−μs) motion. Exchange experiments are sensitive to slow motional processes (>1 ms) when the chemical shifts of resonances for differents conformers are resolved. Motion faster than 1 μs averages the anisotropic nuclear spin interactions. The amplitude of the motional process can thus be estimated from experiments that reintroduce the ^{1}H,^{13}C, or ^{1}H,^{15}N dipolar couplings, e.g., in DIPSHIFT experiments.[172−175] CPPI type experiments are insensitive with respect to remote protons and yield improved performance in comparison to the noncompensated sequences.[176−178] CPPI is, however, affected by RF inhomogeneities on the RF channel that is employed to switch between the matching conditions.[179] Alternatively, REDOR can be employed instead of CPPI, if remote protons can be depleted as in perdeuterated samples.[179−181] A further possibility to determine the motional amplitude at a given site are off-magic-angle spinning experiments with angle offsets as small as 0.03°.[182,183] At 100 kHz MAS, motionally averaged dipolar couplings can be determined using variable-contact CP.[184]

To quantitatively describe dynamics, the extended model-free formalism has been introduced.[185] At least four observables are needed to yield a quantitative description of motion on two time scales and to fit motional amplitudes and correlation times. For the fit of the data for α-SH3,[82] a combination of ^{15}N-R_1 relaxation rates measured at different fields,[186,187] ^{1}H−^{15}N dipole, ^{15}N-CSA cross-correlated relaxation rates η,[74,188,189] as well as CPPI derived dipolar order parameters[190] were employed. Spin diffusion can potentially affect the quantification

https://doi.org/10.1021/acs.chemrev.1c00681
Chem. Rev. XXXX, XXX, XXX−XXX

of R_1 relaxation rates.[187,191,192] If magnetization flows to remote nuclei, e.g., to methyl groups which have a short relaxation time, the relaxation rate will appear systematically larger. Cross-correlated relaxation rates η yield frequency independent spectral density functions, similar to transversal R_2 rates in solution. As an alternative, $R_{1\rho}$ rates can be analyzed to yield site-specific incoherent R_2 type relaxation rates.[193] Depending on the resonance offset, $R_{1\rho}$ depends on a combination of R_1, R_2, and the exchange rate in case slow motional processes are involved. In principle, the number of observables can be increased if relaxation parameters measured for neighboring nuclei are taken into account. Lamley et al. have shown that the motion of the peptide plane can be modeled from combined backbone ^{15}N amide and ^{13}C′ carbonyl data.[194] This allows increase of the number of time scales in the extended model free analysis. Using this extended model-free formalism,[185] the dynamics of the α-spectrin SH3 domain,[82] ubiquitin,[195,196] and superoxide dismutase[153] were quantified. Similarly, backbone dynamics was characterized for the D76N mutant of β-2 microglobulin.[197] R_1, $R_{1\rho}$, and order parameters were employed to quantify dynamics in an extended model-free analysis. It was shown that the outer strands of D76N β2m are destabilized accounting for the increased aggregation propensity of this mutant. Site-specific R_1, $R_{1\rho}$, and order parameters via REDOR have been measured further for the backbone ^{15}N and ^{13}C$^{\alpha}$ nuclei for fibrils of the fungal prion protein HET-s(218−289).[198] The ^{15}N and ^{13}C$^{\alpha}$ data were fit, assuming motions at three time scales which provides a statistically significant, better fit of the relaxation data. There, a slow correlation time of 6.2 μs for ^{1}H−^{15}N, and 4.1 μs for ^{13}C$^{\alpha}$ ^{1}H$^{\alpha}$−^{13}C$^{\alpha}$ are obtained, indicating the presence of a slow global fibril motion. The associated order parameters are very high, with $S_S^2 \geq 0.98$.

The dilemma with the analysis of relaxation rates in the solid state lies in the problem that R_1 spin−lattice relaxation rates are determined not only by incoherent effects, i.e., structural fluctuations, but to a large extent also by coherent interactions that are dependent on the local spin density. Care has to be taken to disentangle the involved coherent and incoherent effects. Isolated nuclei are in principle ideally suited to quantify dynamics because inhomogeneous interactions are more easily refocused. Spin diffusion, e.g., during a relaxation period, results in homonuclear magnetization transfer and yields an apparently shorter ^{13}C T_1 relaxation time in case a nucleus is interacting with, e.g., a methyl group which has a short relaxation time and basically acts as a "sink" for magnetization.[199] For a correct analysis of backbone C$^{\alpha}$ carbon relaxation rates, dilution of both the proton and carbon spin system together with fast MAS are thus important.[200] A dilution of the carbon spin system can be achieved by growing the protein in a M9 minimal medium that employs [μ-^{2}H, 2-^{13}C]- or [μ-^{2}H, 1,3-^{13}C]-glycerol as the sole carbon source. To introduce protons sporadically, the medium contains low amounts of H_2O.[39] A set of MAS dependent relaxation measurements show that both proton and carbon spin dilution are necessary to yield a MAS independent and monoexponential, e.g., ^{13}C-T_1 relaxation decay curves. Alternatively, selective methyl labeling allows to incorporate an isolated carbon spin into the protein.[32]

In the Lipari−Szabo model-free approach, motion is described by employing a sum of spectral density functions. Each term of the sum reflects a linear independent motional regime and contains an order parameter and a correlation time. Smith et al.[201] hypothesize that the fit might be distorted, and specifically those correlation times are obtained where relaxation experiments are particularly sensitive. The model-free approach requires linear independent motional regimes. If dynamics are more complex, the model-free approach breaks down. This induces a bias in the resulting dynamics description. It was therefore suggested to employ so-called "dynamics detectors", which characterize different ranges of correlation times. In this approach, no specific model for the correlation function is needed any longer to analyze protein motion.

Rotating-frame relaxation rates ($R_{1\rho}$) rates can be exploited further to probe micro- to millisecond time scale motions.[202−204] $R_{1\rho}$ measurements have been employed to analyze protein rocking motions in crystals.[205−208] At low RF field strengths in the $R_{1\rho}$ experiment, isotropic chemical shift fluctuation induce the relaxation dispersion that are familiar from solution-state NMR. When the effective RF field ω_e approaches the rotary resonance condition ($\omega_e \simeq n \times \omega_r$, with n = 1,2) bond angle fluctuations induce an increased $R_{1\rho}$ rate reflecting fluctuations of anisotropic interactions. This condition is referred to as near-rotary-resonance $R_{1\rho}$ relaxation-dispersion (NERRD) and can be exploited in a complementary way to retrieve information on the chemical shift differences between the two states, the amplitude of the motion, the populations, and the involved exchange rates.[207,209,210] Using this method, the relaxation dispersion profiles for both the Bloch−McConnell and the near-rotary resonance regimes were modeled for fibrils formed by the human prion protein Y145Stop. Under the assumption of a two-state exchange mechanism, the amino acids of the fibril core exchange with a rate on the order of 1000 s^{-1} with a population of the excited state of 2%.[211] Similarly to ^{15}N $R_{1\rho}$, also ^{1}H $R_{1\rho}$ relaxation-dispersion can be measured for highly deuterated protein samples.[212,213] While ^{15}N $R_{1\rho}$ relaxation rates rather sense local fluctuations, ^{1}H $R_{1\rho}$ is a sensor of more global structural rearrangements due to its higher gyromagnetic ratio. Using these experiments, loop motions have been observed, suggesting that the protein adopts a binding-competent conformation in dynamic equilibrium with a sterically impaired ground-state conformation both in solution and in its crystalline form.

Additional information on the underlying motional model can come from heteronuclear NOE experiments. A significant heteronuclear NOE is expected for side chain methyl and amino groups due their fast 3-fold rotation which results in a fluctuation of the effective dipolar coupling at the respective heteronucleus and thus in relaxation. The heteronuclear NOE in combination with cross-polarization can be exploited for polarization transfer.[214] This has subsequently been applied to proteins.[215−217] Heteronuclear NOEs for amide nitrogens in the protein backbone in the solid state were observed first by Giraud et al.[218] Site-specific [^{1}H]^{13}C and [^{1}H]^{15}N heteronuclear NOE rates for methyl and amide backbone as well as for side chain groups were quantified by Lopez del Amo and co-workers.[219] The heteronuclear NOE is sensitive only to very fast time scale motion and enables the detection of motional processes with a picosecond correlation time. The low sensitivity of the experiment, however, prevents a more detailed quantitative analysis. More recently, the heteronuclear NOE involving methyls has been exploited in high-field DNP experiments[220] as a dynamic sensors for probing local molecular packing and to selectively enhance the polarization of nuclei of residues within the ligand-binding pocket.

MD simulations can help to visualize motion and to get quantitative motional models. For the α-spectrin SH3 domain-, solution,- and solid-state NMR derived order parameters were

https://doi.org/10.1021/acs.chemrev.1c00681
Chem. Rev. XXXX, XXX, XXX−XXX

quantified and compared to a MD trajectory to quantify the amplitude and time scale of backbone motion.[221] It was found that in α-spectrin SH3 ns−μs motions occur in dynamic loops, termini, and side chains, but generally not in the structured portion of the backbone. Similarly, combination of relaxation data and MD simulations allowed to characterize the dynamics of fibrils of the fungal prion protein HET-s(218−289).[222] Here, the NMR data were subjected to the dynamics detector method. From the MD trajectory, cross-correlation coefficients were extracted to find out whether motion of different residues occurs on the same time scale in a correlated way. It was found that local motions occur typically on short time scales, while for longer-range correlated motion take place on longer time scales. Grohe et al. compared MD simulations, NMR relaxation measurements, and an eNOE-based structural ensemble approach for the chicken α-spectrin SH3 domain. The combined analysis showed that the data are consistent with respect to both the time scales and the conformational states that are sampled in the dynamic MD trajectory.[223]

In the following, a few examples shall be given in which efforts have been made to quantify amplitude and time scale for different biomolecular systems. For ubiquitin, 1 μs time scale motion has been observed for the entire protein. Most residues displayed small-amplitude motion, while larger-amplitude dynamics were observed for the β1−β2 turn and the N terminus of the α-helix.[224] For the β-barrel OmpA, ^{1}H−^{15}N dipolar coupling as well as ^{15}N R_1 and $R_{1\rho}$ relaxation rates at fast (60 kHz) MAS and high magnetic field (1 GHz) were measured to describe the motion site specifically.[225] It has been suggested that motion occurs as a collective rocking motion of low amplitude and of hundreds of nanoseconds time scale. Enhanced ^{15}N $R_{1\rho}$ relaxation rates observed for residues located at the edges of the strands suggest an increased mobility of the connecting loops. By determining the de novo NMR structure of the membrane protein AlkL in lipid bilayers and by accessing structural dynamics in combination with MD simulations, MAS solid-state NMR experiments allowed to solve the controversy between crystal and NMR structures of homologues of this protein.[226,227] It was found that dynamic lateral exit sites occur through restructuring of a barrel extension formed by the extracellular loops. Investigations of the fully mature functional Cu, Zn state of superoxide dismutase and its E, Zn-state in which the Cu site is empty have shown that the metal ion after uptake does not act as a rigidification element. Using ^{15}N R_1, $R_{1\rho}$ experiments, it has been shown that metal binding acts rather as a switch that redistributes motional processes on different time scales and induces a coupling of the dynamics of the histidine side chains to remote key backbone elements of the protein.[228] The SAIL approach allows selectivity of isotopically labeled aromatic rings in proteins.[160] This labeling in combination with ^{1}H detected experiments yielded the quantification of motional amplitudes and rates of phenylalanine side chain dynamics in the half-megadalton enzyme complex, aminopeptidase TET2.[161] In the past, carbonic anhydrase II was considered to be a prototypical rigid drug target. While X-ray crystallography has suggested that CA-II has little structural plasticity, MAS solid-state NMR could demonstrate that the binding pocket undergoes pronounced open/close conformational-exchange dynamics, which are abrogated upon binding of a sulfonamide inhibitor.[229,230] ^{1}H detection is further employed in ligand titration experiments to find out how the ClpP protease machinery is activated by substrates or blocked by active-site inhibitors.[231]

11. MOTIONAL INTERFERENCE WITH DECOUPLING

The investigations of protein dynamics in the solid state described above are not purely academic but are of fundamental practical importance. Local dynamics in the ns−μs regime with a significant amplitude will have detrimental effects on the quality of the obtained correlation spectra recorded with high-power decoupling. Averaging of H^{α}/H^{β} spin states results then in a broadening of the observed, e.g., ^{15}N resonances if the respective amide moiety undergoes large amplitude ns−μs motion. Similarly, proton resonances also would be broadened in case the heteronuclear spin is decoupled.[232] This effect was observed for several residues in the α-spectrin SH3 domain. which have a local correlation time on the order of several hundred nanoseconds.[74,233] For these residues, it turns out that TROSY[234] like experiments yield spectroscopic advantages. In fact, broad proton lines were observed previously for fibrils of perdeuterated Alzheimer's disease Aβ40.[52,235] For fibrils of α-synuclein fibrils[26] and hydrophobins,[236] a similar spectral quality is obtained. Spin-state selective excitation and transfer experiments in principle allow to observe the narrow multiplet component. However, so far, no beneficial effects from TROSY type experiments have been observed for amyloid fibrils or membrane proteins in the solid state.[87]

12. SEDIMENTED SOLUTIONS

In addition to classical biological solids such as amyloid fibrils and membrane proteins, MAS solid-state NMR allows to investigate high molecular weight protein complexes in solution. To achieve refocusing of anisotropic interactions by magic angle spinning, the tumbling correlation time of the protein in the rotor must exceed the rotor period.[237] In a typical MAS solid-state NMR experiment, rotation of the sample induces accelerations due to centrifugation on the order of 1−10 × 10^6 g.[238,239] Depending on its molecular weight, sedimentation efficiently immobilizes the soluble protein. Essential for the success of the method is the development of packing tools that allow efficient transfer of protein material into the solid-state NMR rotor.[240−245] Using this approach, the 20S proteasome,[246] the 50S ribosome,[247,248] the 50S bound trigger factor,[249] and immunoglobulins in complex with GB1[60] have been investigated. Small heat shock proteins such as αB-crystallin assemble into oligomers with a molecular weight of 400−600 kDa. These complexes are too heterogeneous and dynamic to form stable crystals that can be analyzed with X-ray crystallography.[250] Misfolding peptides and proteins interact with the chaperones and form chaperone−substrate complexes in the MDa range. These substrate complexes remain in solution, in contrast to the pure substrates that aggregate and precipitate. Traditionally, protein complexes are crystallized using a precipitant such as polyethylene glycol (PEG).[251] This procedure prevents the investigation of chaperone−substrate complexes as the interaction between the small heat shock protein and the amyloidogenic substrate is very weak. MAS solid-state NMR is as such the perfect tool to investigate chaperone−amyloid complexes: MAS solid-state NMR allows overcoming of the limitations of NMR imposed by the tumbling of the proteins in solution. At the same time, sedimentation is not irreversible, but samples can be recovered after the experiment. The investigations can be carried out in a native-like environment without the need to irreversibly precipitate the sample.

Immobilization of protein complexes by sedimentation enabled furthermore the investigation of transient complexes

https://doi.org/10.1021/acs.chemrev.1c00681
Chem. Rev. XXXX, XXX, XXX−XXX

formed by the 177 residue homotetrameric single-stranded DNA binding protein SSB with the single-stranded DNA that is involved in regulation of *Escherichia coli* DNA metabolism.[252] Using proton-detected solid-state NMR experiments, the binding site of the inhibitor bortezomib could be identified at an active-site residue on the 14-subunit complex of caseinolytic protease ClpP.[231] Finally, the method allows to study membraneless cellular organelles, liquid−liquid phase separation, and hydrogels.[253]

13. CONSEQUENCES OF DEUTERATION ON PROTEIN STABILITY, ENZYMATIC ACTIVITY, AND FUNCTION

Deuteration can in principle affect the chemical properties of a protein. It has been shown that D_2O and thus replacing protons by deuterons at exchangeable sites has a stabilizing effect on the protein structure.[254−256] On the other hand, substitution of protons with deuterons at nonexchanageble sites decreases the hydrophobic effect,[257,258] and this way potentially increases dynamics within the hydrophobic core of a protein. For transthyretin, it has been shown that deuteration influences subunit exchange and accelerates its aggregation kinetics.[259] Similarly, the hydrophobic effect can affect the activity of an enzyme.[260] Other reports have shown, however, that enzyme activity is not affected by deuteration.[261,262] In any case, care should be taken and the macroscopic properties of protonated and deuterated samples have to be compared in order to rule out systematic errors in the analysis.

14. FASTER MAS, HIGHER FIELDS, AND PROTONATED SAMPLES

Initially, proton detected experiments were carried out using perdeuterated samples in which 20% of the exchangeable sites were protonated.[25,79] The employed 3.2 mm rotors achieve rotation frequencies on the order of 10−20 kHz and can accommodate 40 μL of sample. Faster MAS has historically led to higher quality and more informative solid-state NMR spectra. An increase of the MAS rotation frequency to 60 kHz was sufficient to increase the proton concentration so that 100% of all exchangeable sites could be protonated without loss of resolution in the proton dimension.[78,263] The 1.3 mm rotor, which is necessary to achieve a rotation frequency of 60 kHz, can only be filled with 4 μL of material and thus 10× less sample. The anticipated loss in sensitivity is more than compensated with the 5× increase of the labeling density at exchangeable sites and the 2.5× higher quality factor of the NMR coil, which increases with the inverse of the diameter. The effective sensitivity of the 1.3 mm rotor is thus actually 25% larger than the sensitivity achieved by a 3.2 mm rotor despite the fact that only 10% of the material is used. Using a 0.7 mm MAS rotor and rotation frequencies around 110 kHz enable the analysis of a fully protonated sample.[3] The active volume of a 0.7 mm rotor amounts to ca. 0.4 μL. Under these conditions, the absolute intensity of an amide proton resonance from a protonated protein will be lower than the respective intensity from a perdeuterated samples in a 1.3 mm rotor, as the proton concentration at a particular site cannot be increased further. However, the 0.7 mm coil has a 2× improved coil efficiency. At the same time, T_2' and $T_{1\rho}$ increase in smaller rotors,[111] which compensates for some of the losses implicated by the smaller rotor volumes.

The maximum MAS frequency is achieved if the rotor surface approaches the speed of sound.[264] Thus, higher MAS frequencies can only be achieved if the rotor diameter decreases. In the future, faster MAS can potentially be achieved by making use of rotors that have a different geometry[265] or by employing gases that are less viscous than nitrogen. However, the latter point remains to be shown because the strength of the ceramic material has to increase together with the rotation frequency. Ultrafast MAS experiments are potentially interesting for applications, where it is difficult to produce large amount of labeled and reconstituted protein in case the overall sensitivity does not suffer. Faster rotation yields better averaging of proton dipolar interactions. Recently, an experimental MAS frequency dependent intensity analysis for the fully protonated proteins ubiquitin, Rpo4/7, HET-s(218−289), and Cp149 was carried out.[266,267] Comparison of proton solid-state NMR spectra recorded at 100 and 150 kHz MAS shows that the average proton homogeneous line width is reduced by a factor of 1.5, while the experimental line width is decreased by a factor 1.25.[267] At the same time, the sensitivity of an HN correlation experiment is increased by a factor of 1.48. This factor accounts for differences in the efficiencies of the polarization transfer steps, the sample volumes, and coil efficiencies of the two probes as well as line narrowing by MAS.

Direct observation of protons and development of fast spinning probes raises the question which maximum MAS frequency is actually required to achieve the optimum sensitivity for a particular (protonated) sample. For a highly deuterated protein sample in which only methyl groups are selectively protonated, the MAS rotation frequency that is required to yield half of the maximum possible sensitivity ranges from 20 kHz up to 324 kHz, depending on the specific site with an average value of (135 ± 88) kHz at a magnetic field strength of 11.7 T (500 MHz).[38] In case a sensitivity is supposed to be reached that corresponds to 80% of the maximum possible sensitivity, a MAS rotation frequency of (498 ± 370) kHz is necessary. It is easy to imagine that much higher rotation frequencies are necessary to achieve the same intensity for a protonated protein sample.

To appreciate the effect of the proton density on the proton spectral quality, microcrystalline perdeuterated protein samples have been investigated in which protons were selectively introduced into methyl groups.[38] Specifically, methyl groups were labeled either as CH_3, CH_2D, or CHD_2 isotopomers. This allows to modulate the proton density in the protein. Subsequently, the MAS frequency dependent cross peak intensities of the experimental and theoretical spectra was analyzed. It was found that the break-even point, i.e., the MAS frequency that is necessary to reach equal intensity in CH_3 versus CHD_2 selectively methyl protonated samples is dependent on the specific methyl group and is achieved on average at a MAS frequency of (75 ± 53) kHz assuming a B_0 field of 1 GHz. Similarly, on average, a MAS frequency of (41 ± 28) kHz is necessary to achieve the same intensity for CH_2D versus CHD_2 selectively methyl protonated samples. This information is potentially of interest for experiments that involve very large, nonsymmetric protein complexes where signal-to-noise is critical and for which any additional increase in sensitivity is essential for the success of the experiment.[60,247−249]

In the past, more powerful magnets and higher frequency MAS has given access to new areas of research. Novel superconducting magnet technology[268,269] made magnetic fields available in the range of 1.2 to 1.5 GHz. Spectral sensitivity scales with $B_0^{3/2}$.[270] For proton resonances in solid proteins, sensitivity gains beyond the $B_0^{3/2}$ factor are expected when the difference of the isotropic chemical shift is larger than the size of the $^1H-^1H$

https://doi.org/10.1021/acs.chemrev.1c00681
Chem. Rev. XXXX, XXX, XXX−XXX

dipolar coupling. In a showcase study, this has been demonstrated for a selectively methyl protonated α-SH3 domain sample in a deuterated background.[271] It is found that for residues which are embedded in a dense proton coupling network, sensitivity is 2-fold larger than what is expected from the canonical field dependence. The gains are largest for methyl groups that experience large proton dipolar couplings and are thus not dependent on instrumental issues that determine the efficiency of the spectrometer, of the probe, and of the polarization transfer. Recent experimental results at 28.2 T (1.2 GHz) suggest that in particular proton detected MAS solid-state NMR experiments benefit dramatically from the increased magnetic field strength.[272,273]

At 110 kHz MAS, deuterated samples (including selectively methyl protonated samples) yield better sensitivity and resolution in comparison to protonated proteins.[274] It remains to be seen which further improvements the recent developments in magnet and probe design will have on the proton spectral quality in MAS solid-state NMR experiments.

AUTHOR INFORMATION

Corresponding Author

Bernd Reif − *Bayerisches NMR Zentrum (BNMRZ) at the Department of Chemistry, Technische Universität München (TUM), 85747 Garching, Germany; Helmholtz-Zentrum München (HMGU), Deutsches Forschungszentrum für Gesundheit und Umwelt, Institute of Structural Biology (STB), 85764 Neuherberg, Germany;* orcid.org/0000-0001-7368-7198; Email: reif@tum.de

Complete contact information is available at: https://pubs.acs.org/10.1021/acs.chemrev.1c00681

Notes

The author declares no competing financial interest.

Biography

Bernd Reif studied Physics and Biochemistry at the Universität Bayreuth. In 1998, he received his Ph.D. at the Universität Frankfurt in Chemistry, where he worked with Christian Griesinger. After a postdoctoral visit in the group of Robert G. Griffin at the Massachusetts Institute of Technology, Cambridge, USA, he was heading an Emmy−Noether research group of the DFG at the Technische Universität München, hosted by Prof. Horst Kessler. From 2003 to 2010, Dr. Reif was appointed as a group leader at the Leibniz-Institut für Molekulare Pharmakologie (FMP) in Berlin. In 2004, he became a professor at the Charité Universitätsmedizin Berlin. In 2010, Dr. Reif accepted an offer from the Department of Chemistry at the Technische Universität München and became coaffiliated at the Helmholtz-Zentrum München in Neuherberg. His research interests involve the development of MAS solid-state NMR methods for the characterization of the structural and dynamical properties of proteins in the solid-state, as well as the application of solution- and solid-state NMR spectroscopy to the study of amyloidogenic peptides and proteins.

ACKNOWLEDGMENTS

B.R. acknowledges support from the Helmholtz-Gemeinschaft, the Deutsche Forschungsgemeinschaft (DFG, grant Re1435).

REFERENCES

(1) Samoson, A.; Tuherm, T.; Gan, Z. High-Field High-Speed MAS Resolution Enhancement in 1H NMR Spectroscopy of Solids. *Solid State Nucl. Magn. Reson.* **2001**, *20*, 130−136.

(2) Samoson, A. H-MAS. *J. Magn. Reson.* **2019**, *306*, 167−172.

(3) Andreas, L. B.; Jaudzems, K.; Stanek, J.; Lalli, D.; Bertarello, A.; Le Marchand, T.; Cala-De Paepe, D.; Kotelovica, S.; Akopjana, I.; Knott, B.; et al. Structure of fully protonated proteins by proton-detected magic-angle spinning NMR. *Proc. Natl. Acad. Sci. U. S. A.* **2016**, *113*, 9187−9192.

(4) Schnabel, B.; Haubenreisser, U.; Scheler, G.; Müller, R. *19th Congress Ampere*, 1976; p 441.

(5) Gerstein, B. C.; Chow, C.; Pembleton, R. G.; Wilson, R. C. Utility of Pulse Nuclear Magnetic Resonance in Studying Protons in Coals. *J. Phys. Chem.* **1977**, *81*, 565−570.

(6) Burum, D. P. Combined Rotation and Multiple Pulse Spectroscopy (CRAMPS). *Concepts Magn. Reson.* **1990**, *2*, 213−227.

(7) Levitt, M. H.; Kolbert, A. C.; Bielecki, A.; Ruben, D. J. High Resolution H-1-NMR in Solids with Frequency-Switched Multiple-Pulse sequences. *Solid State Nucl. Magn. Reson.* **1993**, *2*, 151−163.

(8) Vinogradov, E.; Madhu, P. K.; Vega, S. Proton spectroscopy in solid state nuclear magnetic resonance with windowed phase modulated Lee − Goldburg decoupling sequences. *Chem. Phys. Lett.* **2002**, *354*, 193−202.

(9) Brown, S. P.; Lesage, A.; Elena, B.; Emsley, L. Probing proton-proton proximities in the solid state: High-resolution two-dimensional H-1-H-1 double-quantum CRAMPS NMR spectroscopy. *J. Am. Chem. Soc.* **2004**, *126*, 13230−13231.

(10) Chevelkov, V.; Faelber, K.; Diehl, A.; Heinemann, U.; Oschkinat, H.; Reif, B. Detection of dynamic water molecules in a microcrystalline sample of the SH3 domain of alpha-spectrin by MAS solid-state NMR. *J. Biomol. NMR* **2005**, *31*, 295−310.

(11) Reif, B. Ultra-high resolution in MAS solid-state NMR of perdeuterated proteins: Implications for Structure and Dynamics. *J. Magn. Reson.* **2012**, *216*, 1−12.

(12) LeMaster, D. M.; Richards, F. M. NMR Sequential Assignment of Escherichia Coli Thioredoxin Utilizing Random Fractional Deuteration. *Biochemistry* **1988**, *27*, 142−150.

(13) LeMaster, D. M. Deuteration in protein proton magnetic resonance. *Methods Enzymol.* **1989**, *177*, 23−43.

(14) Kay, L. E.; Gardner, K. H. Solution NMR spectroscopy beyond 25 kDa. *Curr. Opin. Struct. Biol.* **1997**, *7*, 722−731.

(15) McDermott, A. E.; Creuzet, F. J.; Kolbert, A. C.; Griffin, R. G. High-Resolution Magic-Angle-Spinning NMR Spectra of Protons in Deuterated Solids. *J. Magn. Reson.* **1992**, *98*, 408−413.

(16) Zheng, L.; Fishbein, K. W.; Griffin, R. G.; Herzfeld, J. Two-Dimensional Solid-State ^{1}H NMR and Proton Exchange. *J. Am. Chem. Soc.* **1993**, *115*, 6254−6261.

(17) Zorin, V. E.; Brown, S. P.; Hodgkinson, P. Origins of linewidth in 1H magic-angle spinning NMR. *J. Chem. Phys.* **2006**, *125*, 144508.

(18) Reif, B.; Jaroniec, C. P.; Rienstra, C. M.; Hohwy, M.; Griffin, R. G. ^{1}H-^{1}H MAS Correlation Spectroscopy and Distance Measurements in a Deuterated Peptide. *J. Magn. Reson.* **2001**, *151*, 320−327.

(19) Reif, B.; Griffin, R. G. ^{1}H detected ^{1}H,^{15}N Correlation Spectroscopy in Rotating Solids. *J. Magn. Reson.* **2003**, *160*, 78−83.

(20) Zhou, D. H.; Graesser, D. T.; Franks, W. T.; Rienstra, C. M. Sensitivity and resolution in proton solid-state NMR at intermediate deuteration levels: Quantitative linewidth analysis and applications to correlation spectroscopy. *J. Magn. Reson.* **2006**, *178*, 297−307.

(21) Chevelkov, V.; van Rossum, B. J.; Castellani, F.; Rehbein, K.; Diehl, A.; Hohwy, M.; Steuernagel, S.; Engelke, F.; Oschkinat, H.; Reif, B. 1H detection in MAS solid state NMR spectroscopy employing pulsed field gradients for residual solvent suppression. *J. Am. Chem. Soc.* **2003**, *125*, 7788−7789.

(22) Reif, B.; van Rossum, B. J.; Castellani, F.; Rehbein, K.; Diehl, A.; Oschkinat, H. Characterization of ^{1}H ^{1}H distances in a uniformly ^{2}H,^{15}N labeled SH3 domain by MAS solid state NMR spectroscopy. *J. Am. Chem. Soc.* **2003**, *125*, 1488−1489.

(23) Paulson, E. K.; Morcombe, C. R.; Gaponenko, V.; Dancheck, B.; Byrd, R. A.; Zilm, K. W. High-Sensitivity Observation of Dipolar Exchange and NOEs between Exchangeable Protons in Proteins by 3D Solid-State NMR Spectroscopy. *J. Am. Chem. Soc.* **2003**, *125*, 14222−14223.

(24) Paulson, E. K.; Morcombe, C. R.; Gaponenko, V.; Dancheck, B.; Byrd, R. A.; Zilm, K. W. Sensitive High Resolution Inverse Detection NMR Spectroscopy of Proteins in the Solid State. *J. Am. Chem. Soc.* **2003**, *125*, 15831−15836.

(25) Chevelkov, V.; Rehbein, K.; Diehl, A.; Reif, B. Ultra-high resolution in proton solid-state NMR at high levels of deuteration. *Angew. Chem., Int. Ed.* **2006**, *45*, 3878−3881.

(26) Zhou, D. H.; Nieuwkoop, A. J.; Berthold, D. A.; Comellas, G.; Sperling, L. J.; Tang, M.; Shah, G. J.; Brea, E. J.; Lemkau, L. R.; Rienstra, C. M. Solid-state NMR analysis of membrane proteins and protein aggregates by proton detected spectroscopy. *J. Biomol. NMR* **2012**, *54*, 291−305.

(27) Lakomek, N. A.; Frey, L.; Bibow, S.; Böckmann, A.; Riek, R.; Meier, B. H. Proton-Detected NMR Spectroscopy of Nanodisc-Embedded Membrane Proteins: MAS Solid-State vs Solution-State Methods. *J. Phys. Chem. B* **2017**, *121*, 7671−7680.

(28) Niu, Z.; Sarkar, R.; Aichler, M.; Wester, H.-J.; Yousefi, B. H.; Reif, B. Mapping of the binding interface of PET tracer molecules and Alzheimer Disease Aβ fibrils using MAS solid-state NMR. *ChemBioChem* **2020**, *21*, 2495−2502.

(29) Lecoq, L.; Schledorn, M.; Wang, S. S.; Smith-Penzel, S.; Malar, A. A.; Callon, M.; Nassal, M.; Meier, B. H.; Böckmann, A. 100 kHz MAS Proton-Detected NMR Spectroscopy of Hepatitis B Virus Capsids. *Front. Mol. Biosci.* **2019**, *6*, No. 58.

(30) Agarwal, V.; Reif, B. Residual Methyl Protonation in Perdeuterated Proteins for Multidimensional Correlation Experiments in MAS solid-state NMR Spectroscopy. *J. Magn. Reson.* **2008**, *194*, 16−24.

(31) Agarwal, V.; Diehl, A.; Skrynnikov, N.; Reif, B. High Resolution ^{1}H Detected ^{1}H,^{13}C Correlation Spectra in MAS Solid-State NMR using Deuterated Proteins with Selective ^{1}H,^{2}H Isotopic Labeling of Methyl Groups. *J. Am. Chem. Soc.* **2006**, *128*, 12620−12621.

(32) Agarwal, V.; Xue, Y.; Reif, B.; Skrynnikov, N. R. Protein side-chain dynamics as observed by solution- and solid-state NMR: a similarity revealed. *J. Am. Chem. Soc.* **2008**, *130*, 16611−16621.

(33) Huber, M.; Hiller, S.; Schanda, P.; Ernst, M.; Böckmann, A.; Verel, R.; Meier, B. H. A Proton-Detected 4D Solid-State NMR Experiment for Protein Structure Determination. *ChemPhysChem* **2011**, *12*, 915−918.

(34) Andreas, L. B.; Reese, M.; Eddy, M. T.; Gelev, V.; Ni, Q. Z.; Miller, E. A.; Emsley, L.; Pintacuda, G.; Chou, J. J.; Griffin, R. G. Structure and Mechanism of the Influenza A M2(18−60) Dimer of Dimers. *J. Am. Chem. Soc.* **2015**, *137*, 14877−14886.

(35) Goto, N.; Kay, L. E. New developments in isotope strategies for protein solution NMR spectroscopy. *Curr. Opin. Struct. Biol.* **2000**, *10*, 585−592.

(36) Gans, P.; Hamelin, O.; Sounier, R.; Ayala, I.; Dura, M. A.; Amero, C. D.; Noirclerc-Savoye, M.; Franzetti, B.; Plevin, M. J.; Boisbouvier, J. Stereospecific Isotopic Labeling of Methyl Groups for NMR Spectroscopic Studies of High-Molecular-Weight Proteins. *Angew. Chem., Int. Ed.* **2010**, *49*, 1958−1962.

(37) Kerfah, R.; Plevin, M. J.; Sounier, R.; Gans, P.; Boisbouvier, J. Methyl-specific isotopic labeling: a molecular tool box for solution NMR studies of large proteins. *Curr. Opin. Struct. Biol.* **2015**, *32*, 113−122.

(38) Xue, K.; Sarkar, R.; Tosner, Z.; Lalli, D.; Motz, C.; Koch, B.; Pintacuda, G.; Reif, B. MAS dependent sensitivity of different isotopomers in selectively methyl protonated protein samples in solid state NMR. *J. Biomol. NMR* **2019**, *73*, 625−631.

(39) Asami, S.; Schmieder, P.; Reif, B. High resolution 1H-detected solid-state NMR spectroscopy of protein aliphatic resonances: Access to tertiary structure information. *J. Am. Chem. Soc.* **2010**, *132*, 15133−15135.

(40) Asami, S.; Reif, B. Assignment strategies for aliphatic protons in the solid-state in randomly protonated proteins. *J. Biomol. NMR* **2012**, *52*, 31−39.

(41) Asami, S.; Reif, B. Proton-detected solid-state NMR spectroscopy at aliphatic sites: Applications to Crystalline Systems. *Acc. Chem. Res.* **2013**, *46*, 2089−2097.

(42) Asami, S.; Szekely, K.; Schanda, P.; Meier, B. H.; Reif, B. Optimal degree of protonation for 1H detection of aliphatic sites in randomly deuterated proteins as a function of the MAS frequency. *J. Biomol. NMR* **2012**, *54*, 155−168.

(43) Asami, S.; Reif, B. Accessing Methyl Groups in Proteins via 1H-detected MAS Solid-state NMR Spectroscopy Employing Random Protonation. *Sci. Rep.* **2019**, *9*, No. 15903.

(44) Smith, A. A.; Ravotti, F.; Testori, E.; Cadalbert, R.; Ernst, M.; Böckmann, A.; Meier, B. H. Partially-deuterated samples of HET-s(218−289) fibrils: assignment and deuterium isotope effect. *J. Biomol. NMR* **2017**, *67*, 109−119.

(45) Mance, D.; Sinnige, T.; Kaplan, M.; Narasimhan, S.; Daniels, M.; Houben, K.; Baldus, M.; Weingarth, M. An Efficient Labelling Approach to Harness Backbone and Side-Chain Protons in H-1-Detected Solid-State NMR Spectroscopy. *Angew. Chem., Int. Ed.* **2015**, *54*, 15799−15803.

(46) Medeiros-Silva, J.; Mance, D.; Daniels, M.; Jekhmane, S.; Houben, K.; Baldus, M.; Weingarth, M. H-1-Detected Solid-State NMR Studies of Water-Inaccessible Proteins InVitro and InSitu. *Angew. Chem., Int. Ed.* **2016**, *55*, 13606−13610.

(47) Sinnige, T.; Daniels, M.; Baldus, M.; Weingarth, M. Proton Clouds to Measure Long-Range Contacts between Nonexchangeable Side Chain Protons in Solid-State NMR. *J. Am. Chem. Soc.* **2014**, *136*, 4452−4455.

(48) Movellan, K. T.; Najbauer, E. E.; Pratihar, S.; Salvi, M.; Giller, K.; Becker, S.; Andreas, L. B. Alpha protons as NMR probes in deuterated proteins. *J. Biomol. NMR* **2019**, *73*, 81−91.

(49) Agarwal, V.; Linser, R.; Fink, U.; Faelber, K.; Reif, B. Identification of Hydroxyl Protons, Determination of their Exchange Dynamics, and Characterization of Hydrogen Bonding by MAS solid-state NMR Spectroscopy in a Microcrystalline Protein. *J. Am. Chem. Soc.* **2010**, *132*, 3187−3195.

(50) Friedrich, D.; Brunig, F. N.; Nieuwkoop, A. J.; Netz, R. R.; Hegemann, P.; Oschkinat, H. Collective exchange processes reveal an active site proton cage in bacteriorhodopsin. *Commun. Biol.* **2020**, *3*, No. 4.

(51) Friedrich, D.; Perodeau, J.; Nieuwkoop, A. J.; Oschkinat, H. MAS NMR detection of hydrogen bonds for protein secondary structure characterization. *J. Biomol. NMR* **2020**, *74*, 247−256.

(52) Agarwal, V.; Linser, R.; Dasari, M.; Fink, U.; Lopez del Amo, J.-M.; Reif, B. Hydrogen bonding involving side chain exchangeable groups stabilizes amyloid quarternary structure. *Phys. Chem. Chem. Phys.* **2013**, *15*, 12551−12557.

(53) Movellan, K. T.; Wegstroth, M.; Overkamp, K.; Leonov, A.; Becker, S.; Andreas, L. B. Imidazole-Imidazole Hydrogen Bonding in the pH-Sensing Histidine Side Chains of Influenza A M2. *J. Am. Chem. Soc.* **2020**, *142*, 2704−2708.

(54) Zhou, D. H.; Rienstra, C. M. High-Performance Solvent Suppression for Proton-Detected Solid-State NMR. *J. Magn. Reson.* **2008**, *192*, 167−172.

(55) Chevelkov, V.; Xiang, S.; Giller, K.; Becker, S.; Lange, A.; Reif, B. Perspectives for sensitivity enhancement in proton-detected solid-state NMR of highly deuterated proteins by preserving water magnetization. *J. Biomol. NMR* **2015**, *61*, 151−160.

(56) Wickramasinghe, N. P.; Kotecha, M.; Samoson, A.; Past, J.; Ishii, Y. Sensitivity enhancement in C-13 solid-state NMR of protein microcrystals by use of paramagnetic metal ions for optimizing H-1 T-1 relaxation. *J. Magn. Reson.* **2007**, *184*, 350−356.

(57) Linser, R.; Chevelkov, V.; Diehl, A.; Reif, B. Sensitivity Enhancement Using Paramagnetic Relaxation in MAS Solid State NMR of Perdeuterated Proteins. *J. Magn. Reson.* **2007**, *189*, 209−216.

(58) Wickramasinghe, N. P.; Parthasarathy, S.; Jones, C. R.; Bhardwaj, C.; Long, F.; Kotecha, M.; Mehboob, S.; Fung, L. W.; Past, J.; Samoson, A.; et al. Nanomole-scale protein solid-state NMR by breaking intrinsic H-1 T-1 boundaries. *Nat. Methods* **2009**, *6*, 215−218.

(59) Madl, T.; Bermel, W.; Zangger, K. Use of Relaxation Enhancements in a Paramagnetic Environment for the Structure Determination of Proteins Using NMR Spectroscopy. *Angew. Chem., Int. Ed.* **2009**, *48*, 8259−8262.

https://doi.org/10.1021/acs.chemrev.1c00681
Chem. Rev. XXXX, XXX, XXX−XXX

(60) Oster, C.; Kosol, S.; Hartlmuller, C.; Lamley, J. M.; Iuga, D.; Oss, A.; Org, M. L.; Vanatalu, K.; Samoson, A.; Madl, T.; et al. Characterization of Protein-Protein Interfaces in Large Complexes by Solid-State NMR Solvent Paramagnetic Relaxation Enhancements. *J. Am. Chem. Soc.* **2017**, *139*, 12165−12174.

(61) Linser, R.; Fink, U.; Reif, B. Probing Surface Accessibility of Proteins Using Paramagnetic Relaxation in Solid-State NMR Spectroscopy. *J. Am. Chem. Soc.* **2009**, *131*, 13703−13708.

(62) Asami, S.; Rakwalska-Bange, M.; Carlomagno, T.; Reif, B. Protein−RNA Interfaces Probed by 1H-Detected MAS Solid-State NMR Spectroscopy. *Angew. Chem., Int. Ed.* **2013**, *52*, 2345−2349.

(63) Schutz, A. K.; Soragni, A.; Hornemann, S.; Aguzzi, A.; Ernst, M.; Böckmann, A.; Meier, B. H. The Amyloid-Congo Red Interface at Atomic Resolution. *Angew. Chem., Int. Ed.* **2011**, *50*, 5956−5960.

(64) Yan, S.; Guo, C. M.; Hou, G. J.; Zhang, H. L.; Lu, X. Y.; Williams, J. C.; Polenova, T. Atomic-resolution structure of the CAP-Gly domain of dynactin on polymeric microtubules determined by magic angle spinning NMR spectroscopy. *Proc. Natl. Acad. Sci. U. S. A.* **2015**, *112*, 14611−14616.

(65) Ward, M. E.; Shi, L.; Lake, E.; Krishnamurthy, S.; Hutchins, H.; Brown, L. S.; Ladizhansky, V. Proton-Detected Solid-State NMR Reveals Intramembrane Polar Networks in a Seven-Helical Transmembrane Protein Proteorhodopsin. *J. Am. Chem. Soc.* **2011**, *133*, 17434−17443.

(66) Lalli, D.; Idso, M. N.; Andreas, L. B.; Hussain, S.; Baxter, N.; Han, S.; Chmelka, B. F.; Pintacuda, G. Proton-Based Structural Analysis of a Heptahelical Transmembrane Protein in Lipid Bilayers. *J. Am. Chem. Soc.* **2017**, *139*, 13006−13012.

(67) Najbauer, E. E.; Movellan, K. T.; Schubeis, T.; Schwarzer, T.; Castiglione, K.; Giller, K.; Pintacuda, G.; Becker, S.; Andreas, L. B. Probing Membrane Protein Insertion into Lipid Bilayers by Solid-State NMR. *ChemPhysChem* **2018**, *20*, 302−310.

(68) Oster, C.; Hendriks, K.; Kopec, W.; Chevelkov, V.; Shi, C. W.; Michl, D.; Lange, S.; Sun, H.; de Groot, B. L.; Lange, A. The conduction pathway of potassium channels is water free under physiological conditions. *Sci. Adv.* **2019**, *5*, No. aaw6756.

(69) Shi, C. W.; Oster, C.; Bohg, C.; Li, L. M.; Lange, S.; Chevelkov, V.; Lange, A. Structure and Dynamics of the Rhomboid Protease GlpG in Liposomes Studied by Solid-State NMR. *J. Am. Chem. Soc.* **2019**, *141*, 17314−17321.

(70) Lamley, J. M.; Iuga, D.; Oster, C.; Sass, H. J.; Rogowski, M.; Oss, A.; Past, J.; Reinhold, A.; Grzesiek, S.; Samoson, A.; et al. Solid-State NMR of a Protein in a Precipitated Complex with a FullLength Antibody. *J. Am. Chem. Soc.* **2014**, *136*, 16800−16806.

(71) Lamley, J. M.; Oster, C.; Stevens, R. A.; Lewandowski, J. R. Intermolecular Interactions and Protein Dynamics by Solid-State NMR Spectroscopy. *Angew. Chem., Int. Ed.* **2015**, *54*, 15374−15378.

(72) Movellan, K. T.; Derviş̧oğlu, R.; Becker, S.; Andreas, L. B. Pore-Bound Water at the Key Residue Histidine 37 in Influenza A M2. *Angew. Chem., Int. Ed.* **2021**, *60*, 24075.

(73) Maricq, M. M.; Waugh, J. S. NMR in rotating solids. *J. Chem. Phys.* **1979**, *70*, 3300−3316.

(74) Chevelkov, V.; Faelber, K.; Schrey, A.; Rehbein, K.; Diehl, A.; Reif, B. Differential Line Broadening in MAS solid-state NMR due to Dynamic Interference. *J. Am. Chem. Soc.* **2007**, *129*, 10195−10200.

(75) Agarwal, V.; Faelber, K.; Schmieder, P.; Reif, B. High-Resolution Double-Quantum Deuterium Magic Angle Spinning Solid-State NMR Spectroscopy of Perdeuterated Proteins. *J. Am. Chem. Soc.* **2009**, *131*, 2−3.

(76) Penzel, S.; Smith, A. A.; Ernst, M.; Meier, B. H. Setting the magic angle for fast magic-angle spinning probes. *J. Magn. Reson.* **2018**, *293*, 115−122.

(77) Sarkar, R.; Rodriguez Camargo, D. C.; Pintacuda, G.; Reif, B. Restoring Resolution in Biological Solid-State NMR under Conditions of Off-Magic-Angle Spinning. *J. Phys. Chem. Lett.* **2015**, *6*, 5040−5044.

(78) Lewandowski, J. R.; Dumez, J. N.; Akbey, U.; Lange, S.; Emsley, L.; Oschkinat, H. Enhanced Resolution and Coherence Lifetimes in the Solid-State NMR Spectroscopy of Perdeuterated Proteins under Ultrafast Magic-Angle Spinning. *J. Phys. Chem. Lett.* **2011**, *2*, 2205−2211.

(79) Akbey, U.; Lange, S.; Franks, W. T.; Linser, R.; Rehbein, K.; Diehl, A.; van Rossum, B.-J.; Reif, B.; Oschkinat, H. Optimum Levels of Exchangeable Protons in Perdeuterated Proteins for Proton Detection in MAS Solid-State NMR Spectroscopy. *J. Biomol. NMR* **2010**, *46*, 67−73.

(80) Zhou, D. H.; Shea, J. J.; Nieuwkoop, A. J.; Franks, W. T.; Wylie, B. J.; Mullen, C.; Sandoz, D.; Rienstra, C. M. Solid-State Protein-Structure Determination with Proton-Detected Triple-Resonance 3D Magic-Angle-Spinning NMR Spectroscopy. *Angew. Chem., Int. Ed.* **2007**, *46*, 8380−8383.

(81) Zhou, D. H.; Shah, G.; Cormos, M.; Mullen, C.; Sandoz, D.; Rienstra, C. M. Proton-detected solid-state NMR Spectroscopy of fully protonated proteins at 40 kHz magic-angle spinning. *J. Am. Chem. Soc.* **2007**, *129*, 11791−11801.

(82) Chevelkov, V.; Fink, U.; Reif, B. Quantitative Analysis of Backbone Motion in Proteins using MAS Solid-State NMR Spectroscopy. *J. Biomol. NMR* **2009**, *45*, 197−206.

(83) Vanderhart, D. L.; Earl, W. L.; Garroway, A. N. Resolution in C-13 NMR of Organic-Solids Using High-Power Proton Decoupling and Magic-Angle Sample Spinning. *J. Magn. Reson.* **1981**, *44*, 361−401.

(84) Garroway, A. N. Homogeneous and Inhomogeneous Nuclear Spin Echoes in Organic Solids: Adamantane. *J. Magn. Reson.* **1977**, *28*, 365−371.

(85) Cowans, B. A.; Grutzner, J. B. Examination of homogeneous broadening in solids via rotationally synchronized spin-echo NMR-spectroscopy. *J. Magn. Reson., Ser. A* **1993**, *105*, 10−18.

(86) Wiench, J. W.; Lin, V. S.-Y.; Pruski, M. Si-29 NMR in solid state with CPMG acquisition under MAS. *J. Magn. Reson.* **2008**, *193*, 233−242.

(87) Linser, R.; Sarkar, R.; Krushelnitzky, A.; Mainz, A.; Reif, B. Dynamics in the solid-state: perspectives for the investigation of amyloid aggregates, membrane proteins and soluble protein complexes. *J. Biomol. NMR* **2014**, *59*, 1−14.

(88) Barbet-Massin, E.; Pell, A. J.; Retel, J. S.; Andreas, L. B.; Jaudzems, K.; Franks, W. T.; Nieuwkoop, A. J.; Hiller, M.; Higman, V.; Guerry, P.; et al. Rapid Proton-Detected NMR Assignment for Proteins with Fast Magic Angle Spinning. *J. Am. Chem. Soc.* **2014**, *136*, 12489−12497.

(89) Vasa, S. K.; Singh, H.; Grohe, K.; Linser, R. Assessment of a Large Enzyme-Drug Complex by Proton-Detected Solid-State NMR Spectroscopy without Deuteration. *Angew. Chem., Int. Ed.* **2019**, *58*, 5758−5762.

(90) Fricke, P.; Chevelkov, V.; Zinke, M.; Giller, K.; Becker, S.; Lange, A. Backbone assignment of perdeuterated proteins by solid-state NMR using proton detection and ultrafast magic-angle spinning. *Nat. Protoc.* **2017**, *12*, 764−782.

(91) Penzel, S.; Smith, A. A.; Agarwal, V.; Hunkeler, A.; Org, M. L.; Samoson, A.; Böckmann, A.; Ernst, M.; Meier, B. H. Protein resonance assignment at MAS frequencies approaching 100 kHz: a quantitative comparison of J-coupling and dipolar-coupling-based transfer methods. *J. Biomol. NMR* **2015**, *63*, 165−186.

(92) Linser, R.; Fink, U.; Reif, B. Proton-detected Scalar Coupling based Assignment Strategies in MAS Solid-State NMR Spectroscopy applied to Perdeuterated Proteins. *J. Magn. Reson.* **2008**, *193*, 89−93.

(93) Linser, R.; Fink, U.; Reif, B. Narrow carbonyl resonances in proton-diluted proteins facilitate NMR assignments in the solid-state. *J. Biomol. NMR* **2010**, *47*, 1−6.

(94) Schanda, P.; Huber, M.; Verel, R.; Ernst, M.; Meier, B. H. Direct Detection of 3hJNC Hydrogen-Bond Scalar Couplings in Proteins by Solid-State NMR Spectroscopy. *Angew. Chem., Int. Ed.* **2009**, *48*, 9322−9325.

(95) Chevelkov, V.; Giller, K.; Becker, S.; Lange, A. Efficient CO-CA transfer in highly deuterated proteins by band-selective homonuclear cross-polarization. *J. Magn. Reson.* **2013**, *230*, 205−211.

(96) Chevelkov, V.; Habenstein, B.; Loquet, A.; Giller, K.; Becker, S.; Lange, A. Proton-detected MAS NMR experiments based on dipolar

https://doi.org/10.1021/acs.chemrev.1c00681
Chem. Rev. XXXX, XXX, XXX−XXX

transfers for backbone assignment of highly deuterated proteins. *J. Magn. Reson.* **2014**, *242*, 180−188.

(97) Xiang, S.; Grohe, K.; Rovó, P.; Vasa, S. K.; Giller, K.; Becker, S.; Linser, R. Sequential backbone assignment based on dipolar amide-to-amide correlation experiments. *J. Biomol. NMR* **2015**, *62*, 303−311.

(98) Andreas, L. B.; Stanek, J.; Le Marchand, T.; Bertarello, A.; Cala-De Paepe, D.; Lalli, D.; Krejčíková, M.; Doyen, C.; Öster, C.; Knott, B.; et al. Protein residue linking in a single spectrum for magic-angle spinning NMR assignment. *J. Biomol. NMR* **2015**, *62*, 253−261.

(99) Vasa, S. K.; Singh, H.; Rovó, P.; Linser, R. Dynamics and Interactions of a 29 kDa Human Enzyme Studied by Solid-State NMR. *J. Phys. Chem. Lett.* **2018**, *9*, 1307−1311.

(100) Volk, J.; Herrmann, T.; Wuthrich, K. Automated sequence-specific protein NMR assignment using the memetic algorithm MATCH. *J. Biomol. NMR* **2008**, *41*, 127−138.

(101) Dutta, S. K.; Serrano, P.; Proudfoot, A.; Geralt, M.; Pedrini, B.; Herrmann, T.; Wuthrich, K. APSY-NMR for protein backbone assignment in high-throughput structural biology. *J. Biomol. NMR* **2015**, *61*, 47−53.

(102) Linser, R. Side-chain to backbone correlations from solid-state NMR of perdeuterated proteins through combined excitation and long-range magnetization transfers. *J. Biomol. NMR* **2011**, *51*, 221−226.

(103) Linser, R. Backbone assignment of perdeuterated proteins using long-range H/C-dipolar transfers. *J. Biomol. NMR* **2012**, *52*, 151−158.

(104) Baldus, M.; Meier, B. H. Total correlation spectroscopy in the solid state. The use of scalar couplings to determine the through-bond connectivity. *J. Magn. Reson., Ser. A* **1996**, *121*, 65−69.

(105) Kramer, F.; Peti, W.; Griesinger, C.; Glaser, S. J. Optimized homonuclear Carr-Purcell-type dipolar mixing sequences. *J. Magn. Reson.* **2001**, *149*, 58−66.

(106) Kulminskaya, N.; Vasa, S. K.; Giller, K.; Becker, S.; Kwan, A.; Sunde, M.; Linser, R. Access to side-chain carbon information in deuterated solids under fast MAS through non-rotor-synchronized mixing. *Chem. Commun.* **2016**, *52*, 268−271.

(107) Franks, W. T.; Atreya, H. S.; Szyperski, T.; Rienstra, C. M. GFT projection NMR spectroscopy for proteins in the solid state. *J. Biomol. NMR* **2010**, *48*, 213−223.

(108) Hiller, S.; Fiorito, F.; Wuthrich, K.; Wider, G. Automated projection spectroscopy (APSY). *Proc. Natl. Acad. Sci. U. S. A.* **2005**, *102*, 10876−10881.

(109) Hiller, S.; Wider, G.; Wuthrich, K. APSY-NMR with proteins: practical aspects and backbone assignment. *J. Biomol. NMR* **2008**, *42*, 179−195.

(110) Klein, A.; Vasa, S. K.; Linser, R. Automated projection spectroscopy in solid-state NMR. *J. Biomol. NMR* **2018**, *72*, 163−170.

(111) Orton, H. W.; Stanek, J.; Schubeis, T.; Foucaudeau, D.; Ollier, C.; Draney, A. W.; Le Marchand, T.; Cala-De Paepe, D.; Felli, I. C.; Pierattelli, R.; et al. Protein NMR Resonance Assignment without Spectral Analysis: 5D SOlid-State Automated Projection SpectroscopY (SO-APSY). *Angew. Chem., Int. Ed.* **2020**, *59*, 2380−2384.

(112) Xiang, S. Q.; Chevelkov, V.; Becker, S.; Lange, A. Towards automatic protein backbone assignment using proton-detected 4D solid-state NMR data. *J. Biomol. NMR* **2014**, *60*, 85−90.

(113) Fraga, H.; Arnaud, C. A.; Gauto, D. F.; Audin, M.; Kurauskas, V.; Macek, P.; Krichel, C.; Guan, J. Y.; Boisbouvier, J.; Sprangers, R.; et al. Solid-State NMR H-N-(C)-H and H-N-C-C 3D/4D Correlation Experiments for Resonance Assignment of Large Proteins. *ChemPhysChem* **2017**, *18*, 2697−2703.

(114) Lalli, D.; Schanda, P.; Chowdhury, A.; Retel, J.; Hiller, M.; Higman, V. A.; Handel, L.; Agarwal, V.; Reif, B.; van Rossum, B.-J.; et al. Three-dimensional deuterium-carbon correlation experiments for high-resolution solid-state MAS NMR spectroscopy of large proteins. *J. Biomol. NMR* **2011**, *51*, 477−485.

(115) Vega, S.; Shattuck, T. W.; Pines, A. Fourier Transform Double Quantum NMR in Solids. *Phys. Rev. Lett.* **1976**, *37*, 43−46.

(116) Greenfield, M. S.; Ronemus, A. D.; Vold, R. L.; Vold, R. R.; Ellis, P. D.; Raidy, T. E. Deuterium quadrupole-echo NMR-spectroscopy. 3. Practical aspects of lineshape calculations for multiaxis rotational processes. *J. Magn. Reson.* **1987**, *72*, 89−107.

(117) Vold, R. L.; Hoatson, G. L. Effects of jump dynamics on solid state nuclear magnetic resonance line shapes and spin relaxation times. *J. Magn. Reson.* **2009**, *198*, 57−72.

(118) Spiess, H. W. Molecular dynamics of solid polymers as revealed by deuteron NMR. *Colloid Polym. Sci.* **1983**, *261*, 193−209.

(119) Smith, R. L.; Oldfield, E. Dynamic structure of membranes by deuterium NMR. *Science* **1984**, *225*, 280−288.

(120) Petrache, H. I.; Dodd, S. W.; Brown, M. F. Area per lipid and acyl length distributions in fluid phosphatidylcholines determined by H-2 NMR spectroscopy. *Biophys. J.* **2000**, *79*, 3172−3192.

(121) Gall, C. M.; Cross, T. A.; DiVerdi, J. A.; Opella, S. J. Protein Dynamics by Solid-State NMR: Aromatic Rings of the Coat Protein in fd Bacteriophage. *Proc. Natl. Acad. Sci. U. S. A.* **1982**, *79*, 101−105.

(122) Vugmeyster, L. Recent developments in deuterium solid-state NMR for the detection of slow motions in proteins. *Solid State Nucl. Magn. Reson.* **2021**, *111*, No. 101710.

(123) Hologne, M.; Faelber, K.; Diehl, A.; Reif, B. Characterization of Dynamics of Perdeuterated Proteins by MAS Solid-State NMR. *J. Am. Chem. Soc.* **2005**, *127*, 11208−11209.

(124) Hologne, M.; Chevelkov, V.; Reif, B. Deuteration of Peptides and Proteins in MAS Solid-State NMR. *Prog. Nucl. Magn. Reson. Spectrosc.* **2006**, *48*, 211−232.

(125) Shi, X. Y.; Yarger, J. L.; Holland, G. P. H-2-C-13 HETCOR MAS NMR for indirect detection of H-2 quadrupole patterns and spin-lattice relaxation rates. *J. Magn. Reson.* **2013**, *226*, 1−12.

(126) Shi, X. Y.; Rienstra, C. M. Site-Specific Internal Motions in GB1 Protein Microcrystals Revealed by 3D H-2-C-13-C-13 Solid-State NMR Spectroscopy. *J. Am. Chem. Soc.* **2016**, *138*, 4105−4119.

(127) Akbey, U. Dynamics of uniformly labelled solid proteins between 100 and 300 K: A 2D H-2-C-13 MAS NMR approach. *J. Magn. Reson.* **2021**, *327*, No. 106974.

(128) Hologne, M.; Chen, Z.; Reif, B. Characterization of dynamic processes using deuterium in uniformly ^{2}H,^{13}C,^{15}N enriched peptides by MAS solid-state NMR. *J. Magn. Reson.* **2006**, *179*, 20−28.

(129) Reif, B.; Xue, Y.; Agarwal, V.; Pavlova, M. S.; Hologne, M.; Diehl, A.; Ryabov, Y. E.; Skrynnikov, N. R. Protein Side-Chain Dynamics Observed by Solution- and Solid-state NMR: Comparative Analysis of Methyl ^{2}H Relaxation Data. *J. Am. Chem. Soc.* **2006**, *128*, 12354−12355.

(130) Gelenter, M. D.; Wang, T.; Liao, S. Y.; O'Neill, H.; Hong, M. H-2-C-13 correlation solid-state NMR for investigating dynamics and water accessibilities of proteins and carbohydrates. *J. Biomol. NMR* **2017**, *68*, 257−270.

(131) Wei, D.; Akbey, Ü.; Paaske, B.; Oschkinat, H.; Reif, B.; Bjerring, M.; Nielsen, N. C. Optimal 2H Rf Pulses and 2H-13C Cross-Polarization Methods for Solid-State 2H MAS NMR of Perdeuterated Proteins. *J. Phys. Chem. Lett.* **2011**, *2*, 1289−1294.

(132) Akbey, U.; Nieuwkoop, A. J.; Wegner, S.; Voreck, A.; Kunert, B.; Bandara, P.; Engelke, F.; Nielsen, N. C.; Oschkinat, H. Quadruple-Resonance Magic-Angle Spinning NMR Spectroscopy of Deuterated Solid Proteins. *Angew. Chem., Int. Ed.* **2014**, *53*, 2438−2442.

(133) Akbey, U.; Camponeschi, F.; van Rossum, B.-J.; Oschkinat, H. Triple Resonance Cross-Polarization for More Sensitive (13)C MAS NMR Spectroscopy of Deuterated Proteins. *ChemPhysChem* **2011**, *12*, 2092−2096.

(134) Lopez del Amo, J.-M.; Fink, U.; Reif, B. Quantification of Protein Backbone Hydrogen-Deuterium Exchange Rates by MAS solid-state NMR Spectroscopy. *J. Biomol. NMR* **2010**, *48*, 203−212.

(135) Hwang, S.; Oster, C.; Chevelkov, V.; Giller, K.; Lange, S.; Becker, S.; Lange, A. Characterization of H/D exchange in type 1 pili by proton-detected solid-state NMR and molecular dynamics simulations. *J. Biomol. NMR* **2019**, *73*, 281−291.

(136) Lopez, J.; Ahuja, P.; Landrieu, I.; Cantrelle, F. X.; Huvent, I.; Lippens, G. H/D exchange of a N-15 labelled Tau fragment as measured by a simple Relax-EXSY experiment. *J. Magn. Reson.* **2014**, *249*, 32−37.

(137) Chevelkov, V.; Giller, K.; Becker, S.; Lange, A. Measurement of backbone hydrogen-deuterium exchange in the type III secretion

https://doi.org/10.1021/acs.chemrev.1c00681
Chem. Rev. XXXX, XXX, XXX−XXX

system needle protein PrgI by solid-state NMR. *J. Magn. Reson.* **2017**, *283*, 110−116.

(138) Grohe, K.; Movellan, K. T.; Vasa, S. K.; Giller, K.; Becker, S.; Linser, R. Non-equilibrium hydrogen exchange for determination of H-bond strength and water accessibility in solid proteins. *J. Biomol. NMR* **2017**, *68*, 7−17.

(139) Schmidt-Rohr, K.; Spiess, H. W. Multidimensional Solid-State NMR and Polymers; Academic Press: London, 1994.

(140) Bayro, M. J.; Huber, M.; Ramachandran, R.; Davenport, T. C.; Meier, B. H.; Ernst, M.; Griffin, R. G. Dipolar truncation in magic-angle spinning NMR recoupling experiments. *J. Chem. Phys.* **2009**, *130*, 114506.

(141) LeMaster, D. M.; Kushlan, D. M. Dynamical Mapping of E. coli Thioredoxin via ^{13}C NMR Relaxation Analysis. *J. Am. Chem. Soc.* **1996**, *118*, 9255−9264.

(142) Castellani, F.; van Rossum, B.-J.; Diehl, A.; Schubert, M.; Rehbein, K.; Oschkinat, H. Structure of a protein determined by solid-state magic-angle spinning NMR. *Nature* **2002**, *420*, 99.

(143) De Paepe, G.; Lewandowski, J. R.; Loquet, A.; Böckmann, A.; Griffin, R. G. Proton assisted recoupling and protein structure determination. *J. Chem. Phys.* **2008**, *129*, No. 245101.

(144) Donovan, K. J.; Jain, S. K.; Silvers, R.; Linse, S.; Griffin, R. G. Proton-Assisted Recoupling (PAR) in Peptides and Proteins. *J. Phys. Chem. B* **2017**, *121*, 10804−10817.

(145) Gelenter, M. D.; Dregni, A. J.; Hong, M. Pulsed Third-Spin-Assisted Recoupling NMR for Obtaining Long-Range C-13-C-13 and N-15-C-13 Distance Restraints. *J. Phys. Chem. B* **2020**, *124*, 7138−7151.

(146) Lewandowski, J. R.; De Paepe, G.; Griffin, R. G. Proton assisted insensitive nuclei cross polarization. *J. Am. Chem. Soc.* **2007**, *129*, 728−729.

(147) De Paepe, G.; Lewandowski, J. R.; Loquet, A.; Eddy, M.; Megy, S.; Böckmann, A.; Griffin, R. G. Heteronuclear proton assisted recoupling. *J. Chem. Phys.* **2011**, *134*, No. 095101.

(148) Lee, Y. K.; Kurur, N. D.; Helmle, M.; Johannessen, O. G.; Nielsen, N. C.; Levitt, M. H. Efficient dipolar recoupling in the NMR of rotating solids. A sevenfold symmetric radiofrequency pulse sequence. *Chem. Phys. Lett.* **1995**, *242*, 304−309.

(149) Suter, D.; Ernst, R. R. Spin diffusion in resolved solid-state NMR spectra. *Phys. Rev. B: Condens. Matter Mater. Phys.* **1985**, *32*, 5608−5627.

(150) Bennett, A. E.; Rienstra, C. M.; Griffiths, J. M.; Zhen, W.; Lansbury, P. T., Jr.; Griffin, R. G. Homonuclear Radio Frequency-driven Recoupling in Rotating Solids. *J. Chem. Phys.* **1998**, *108*, 9463−9479.

(151) Verel, R.; Ernst, M.; Meier, B. H. Adiabatic dipolar recoupling in solid-state NMR: The DREAM scheme. *J. Magn. Reson.* **2001**, *150*, 81−99.

(152) Linser, R.; Bardiaux, B.; Higman, V.; Fink, U.; Reif, B. Structure calculation from unambiguous long-range amide and methyl 1H-1H distance restraints for a micro-crystalline protein with MAS solid-state NMR spectroscopy. *J. Am. Chem. Soc.* **2011**, *133*, 5905−5912.

(153) Knight, M. J.; Pell, A. J.; Bertini, I.; Felli, I. C.; Gonnelli, L.; Pierattelli, R.; Herrmann, T.; Emsley, L.; Pintacuda, G. Structure and backbone dynamics of a microcrystalline metalloprotein by solid-state NMR. *Proc. Natl. Acad. Sci. U. S. A.* **2012**, *109*, 11095−11100.

(154) Linser, R.; Bardiaux, B.; Andreas, L. B.; Hyberts, S. G.; Morris, V. K.; Pintacuda, G.; Sunde, M.; Kwan, A. H.; Wagner, G. Solid-State NMR Structure Determination from Diagonal-Compensated, Sparsely Nonuniform-Sampled 4D Proton-Proton Restraints. *J. Am. Chem. Soc.* **2014**, *136*, 11002−11010.

(155) Agarwal, V.; Penzel, S.; Szekely, K.; Cadalbert, R.; Testori, E.; Oss, A.; Past, J.; Samoson, A.; Ernst, M.; Böckmann, A.; et al. De Novo 3D Structure Determination from Sub-milligram Protein Samples by Solid-State 100 kHz MAS NMR Spectroscopy. *Angew. Chem., Int. Ed.* **2014**, *53*, 12253−12256.

(156) Duong, N. T.; Raran-Kurussi, S.; Nishiyama, Y.; Agarwal, V. Can proton-proton recoupling in fully protonated solids provide quantitative, selective and efficient polarization transfer? *J. Magn. Reson.* **2020**, *317*, No. 106777.

(157) Huber, M.; Böckmann, A.; Hiller, S.; Meier, B. H. 4D solid-state NMR for protein structure determination. *Phys. Chem. Chem. Phys.* **2012**, *14*, 5239−5246.

(158) Shi, C. W.; Fricke, P.; Lin, L.; Chevelkov, V.; Wegstroth, M.; Giller, K.; Becker, S.; Thanbichler, M.; Lange, A. Atomic-resolution structure of cytoskeletal bactofilin by solid-state NMR. *Sci. Adv.* **2015**, *1*, No. 1501087.

(159) Xue, K.; Sarkar, R.; Motz, C.; Asami, S.; Decker, V.; Wegner, S.; Tošner, Z.; Reif, B. Magic Angle spinning frequencies beyond 300 kHz are necessary to yield Maximum Sensitivity in Selectively Methyl Protonated protein samples in solid state NMR. *J. Phys. Chem. C* **2018**, *122*, 16437−16442.

(160) Kainosho, M.; Torizawa, T.; Iwashita, Y.; Terauchi, T.; Ono, A. M.; Guntert, P. Optimal isotope labelling for NMR protein structure determinations. *Nature* **2006**, *440*, 52−57.

(161) Gauto, D. F.; Macek, P.; Barducci, A.; Fraga, H.; Hessel, A.; Terauchi, T.; Gajan, D.; Miyanoiri, Y.; Boisbouvier, J.; Lichtenecker, R.; et al. Aromatic Ring Dynamics, Thermal Activation, and Transient Conformations of a 468 kDa Enzyme by Specific H-1-C-13 Labeling and Fast Magic-Angle Spinning NMR. *J. Am. Chem. Soc.* **2019**, *141*, 11183−11195.

(162) Knight, M. J.; Webber, A. L.; Pell, A. J.; Guerry, P.; Barbet-Massin, E.; Bertini, I.; Felli, I. C.; Gonnelli, L.; Pierattelli, R.; Emsley, L.; et al. Fast Resonance Assignment and Fold Determination of Human Superoxide Dismutase by High-Resolution Proton-Detected Solid-State MAS NMR Spectroscopy. *Angew. Chem., Int. Ed.* **2011**, *50*, 11697−11701.

(163) Bennett, A. E.; Ok, J. H.; Griffin, R. G.; Vega, S. Chemical Shift Correlation Spectroscopy in Rotating Solids: Radio-Frequency Dipolar Recoupling and Longitudinal Exchange. *J. Chem. Phys.* **1992**, *96*, 8624−8627.

(164) Retel, J. S.; Nieuwkoop, A. J.; Hiller, M.; Higman, V. A.; Barbet-Massin, E.; Stanek, J.; Andreas, L. B.; Franks, W. T.; van Rossum, B. J.; Vinothkumar, K. R.; et al. Structure of outer membrane protein G in lipid bilayers. *Nat. Commun.* **2017**, *8*, No. 2073.

(165) Grohe, K.; Nimerovsky, E.; Singh, H.; Vasa, S. K.; Soldner, B.; Vogeli, B.; Rienstra, C. M.; Linser, R. Exact distance measurements for structure and dynamics in solid proteins by fast-magic-anglespinning NMR. *Chem. Commun.* **2019**, *55*, 7899−7902.

(166) Knight, M. J.; Felli, I. C.; Pierattelli, R.; Bertini, I.; Emsley, L.; Herrmann, T.; Pintacuda, G. Rapid Measurement of Pseudocontact Shifts in Metalloproteins by Proton-Detected Solid-State NMR Spectroscopy. *J. Am. Chem. Soc.* **2012**, *134*, 14730−14733.

(167) Knight, M. J.; Felli, I. C.; Pierattelli, R.; Emsley, L.; Pintacuda, G. Magic Angle Spinning NMR of Paramagnetic Proteins. *Acc. Chem. Res.* **2013**, *46*, 2108−2116.

(168) Mukhopadhyay, D.; Nadaud, P. S.; Shannon, M. D.; Jaroniec, C. P. Rapid Quantitative Measurements of Paramagnetic Relaxation Enhancements in Cu(II)-Tagged Proteins by Proton-Detected Solid State NMR Spectroscopy. *J. Phys. Chem. Lett.* **2017**, *8*, 5871−5877.

(169) Sengupta, I.; Nadaud, P. S.; Helmus, J. J.; Schwieters, C. D.; Jaroniec, C. P. Protein fold determined by paramagnetic magic-angle spinning solid-state NMR spectroscopy. *Nat. Chem.* **2012**, *4*, 410−417.

(170) Perez, A.; Gaalswyk, K.; Jaroniec, C. P.; MacCallum, J. L. High Accuracy Protein Structures from Minimal Sparse Paramagnetic Solid-State NMR Restraints. *Angew. Chem., Int. Ed.* **2019**, *58*, 6564−6568.

(171) Jirasko, V.; Lends, A.; Lakomek, N. A.; Fogeron, M. L.; Weber, M. E.; Malar, A. A.; Penzel, S.; Bartenschlager, R.; Meier, B. H.; Böckmann, A. Dimer Organization of Membrane-Associated NS5A of Hepatitis C Virus as Determined by Highly Sensitive H-1-Detected Solid-State NMR. *Angew. Chem., Int. Ed.* **2021**, *60*, 5339−5347.

(172) Franks, W. T.; Zhou, D. H.; Wylie, B. J.; Money, B. G.; Graesser, D. T.; Frericks, H. L.; Sahota, G.; Rienstra, C. M. Magic-Angle Spinning Solid-State NMR Spectroscopy of the beta 1 Immunoglobulin Binding Domain of Protein G (GB1): 15N and 13C Chemical Shift Assignments and Conformational Analysis. *J. Am. Chem. Soc.* **2005**, *127*, 12291−12305.

https://doi.org/10.1021/acs.chemrev.1c00681
Chem. Rev. XXXX, XXX, XXX−XXX

(173) Lorieau, J. L.; McDermott, A. E. Order parameters based on (CH)-C-13-H-1, (CH2)-C-13-H-1 and (CH3)-C-13-H-1 heteronuclear dipolar powder patterns: a comparison of MAS-based solid-state NMR sequences. *Magn. Reson. Chem.* **2006**, *44*, 334−347.

(174) Lorieau, J. L.; McDermott, A. E. Conformational Flexibility of a Microcrystalline Globular Protein: Order Parameters by Solid-State NMR Spectroscopy. *J. Am. Chem. Soc.* **2006**, *128*, 11505−11512.

(175) Lorieau, J. L.; Day, L. A.; McDermott, A. E. Conformational dynamics of an intact virus: Order parameters for the coat protein of Pf1 bacteriophage. *Proc. Natl. Acad. Sci. U. S. A.* **2008**, *105*, 10366−10371.

(176) Wu, X. L.; Zilm, K. W. Cross-Polarization with High-Speed Magic-Angle Spinning. *J. Magn. Reson., Ser. A* **1993**, *104*, 154−165.

(177) Dvinskikh, S. V.; Zimmermann, H.; Maliniak, A.; Sandstrom, D. Heteronuclear dipolar recoupling in liquid crystals and solids by PISEMA-type pulse sequences. *J. Magn. Reson.* **2003**, *164*, 165−170.

(178) Dvinskikh, S. V.; Zimmermann, H.; Maliniak, A.; Sandström, D. Heteronuclear dipolar recoupling in solid-state nuclear magnetic resonance by amplitude-, phase-, and frequency-modulated Lee−Goldburg cross-polarization. *J. Chem. Phys.* **2005**, *122*, 044512.

(179) Schanda, P.; Meier, B. H.; Ernst, M. Accurate measurement of one-bond H-X heteronuclear dipolar couplings in MAS solid-state NMR. *J. Magn. Reson.* **2011**, *210*, 246−259.

(180) Schanda, P.; Huber, M.; Boisbouvier, J.; Meier, B. H.; Ernst, M. Solid-State NMR Measurements of Asymmetric Dipolar Couplings Provide Insight into Protein Side-Chain Motion. *Angew. Chem., Int. Ed.* **2011**, *50*, 11005−11009.

(181) Asami, S.; Reif, B. Comparative Study of REDOR and CPPI Derived Order Parameters by 1H-Detected MAS NMR and MD Simulations. *J. Phys. Chem. B* **2017**, *121*, 8719−8730.

(182) Xue, K.; Mühlbauer, M.; Mamone, S.; Sarkar, R.; Reif, B. Accurate Determination of 1H-15N Dipolar Couplings Using Inaccurate Settings of the Magic Angle in Solid-State NMR Spectroscopy. *Angew. Chem., Int. Ed.* **2019**, *58*, 4286−4290.

(183) Xue, K.; Mamone, S.; Koch, B.; Sarkar, R.; Reif, B. Determination of methyl order parameters using solid state NMR under off magic angle spinning. *J. Biomol. NMR* **2019**, *73*, 471−475.

(184) Paluch, P.; Trebosc, J.; Nishiyama, Y.; Potrzebowski, M. J.; Malon, M.; Amoureux, J. P. Theoretical study of CP-VC: A simple, robust and accurate MAS NMR method for analysis of dipolar C-H interactions under rotation speeds faster than ca. 60 kHz. *J. Magn. Reson.* **2015**, *252*, 67−77.

(185) Clore, G. M.; Szabo, A.; Bax, A.; Kay, L. E.; Driscoll, P. C.; Gronenborn, A. M. Deviations from the Simple 2-Parameter Model-Free Approach to the Interpretation of N-15 Nuclear Magnetic Relaxation of Proteins. *J. Am. Chem. Soc.* **1990**, *112*, 4989−4991.

(186) Giraud, N.; Blackledge, M.; Goldman, M.; Böckmann, A.; Lesage, A.; Penin, F.; Emsley, L. Quantitative Analysis of Backbone Dynamics in a Crystalline Protein from Nitrogen-15 Spin-Lattice Relaxation. *J. Am. Chem. Soc.* **2005**, *127*, 18190−18201.

(187) Chevelkov, V.; Diehl, A.; Reif, B. Measurement of ^{15}N-T_1 Relaxation Rates in a Perdeuterated Protein by MAS Solid-State NMR Spectroscopy. *J. Chem. Phys.* **2008**, *128*, 052316.

(188) Chevelkov, V.; Diehl, A.; Reif, B. Quantitative Measurement of Differential ^{15}N-Hα/β T_2 Relaxation Times in a Perdeuterated Protein by MAS Solid-State NMR Spectroscopy. *Magn. Reson. Chem.* **2007**, *45*, S156−S160.

(189) Skrynnikov, N. R. Asymmetric doublets in MAS NMR: coherent and incoherent mechanisms. *Magn. Reson. Chem.* **2007**, *45*, S161−S173.

(190) Chevelkov, V.; Fink, U.; Reif, B. Accurate Determination of Order Parameters from ^{1}H,^{15}N Dipolar Couplings in MAS solid-state NMR experiments. *J. Am. Chem. Soc.* **2009**, *131*, 14018−14022.

(191) Giraud, N.; Blackledge, M.; Böckmann, A.; Emsley, L. The influence of nitrogen-15 proton-driven spin diffusion on the measurement of nitrogen-15 longitudinal relaxation times. *J. Magn. Reson.* **2007**, *184*, 51−61.

(192) Phan, V.; Fry, E. A.; Zilm, K. W. Accounting for the temperature dependence of C-13 spin-lattice relaxation of methyl groups in the glycyl-alanyl-leucine model system under MAS with spin diffusion. *J. Biomol. NMR* **2019**, *73*, 411−421.

(193) Akasaka, K.; Ganapathy, S.; McDowell, C. A.; Naito, A. Spin-Spin and Spin-Lattice Contributions to the Rotating Frame Relaxation of C-13 in L-Alanine. *J. Chem. Phys.* **1983**, *78*, 3567−3572.

(194) Lamley, J. M.; Lougher, M. J.; Sass, H. J.; Rogowski, M.; Grzesiek, S.; Lewandowski, J. R. Unraveling the complexity of protein backbone dynamics with combined C-13 and N-15 solid-state NMR relaxation measurements. *Phys. Chem. Chem. Phys.* **2015**, *17*, 21997−22008.

(195) Schanda, P.; Meier, B. H.; Ernst, M. Quantitative Analysis of Protein Backbone Dynamics in Microcrystalline Ubiquitin by Solid-State NMR Spectroscopy. *J. Am. Chem. Soc.* **2010**, *132*, 15957−15967.

(196) Schanda, P.; Ernst, M. Studying dynamics by magic-angle spinning solid-state NMR spectroscopy: Principles and applications to biomolecules. *Prog. Nucl. Magn. Reson. Spectrosc.* **2016**, *96*, 1−46.

(197) Le Marchand, T.; de Rosa, M.; Salvi, N.; Sala, B. M.; Andreas, L. B.; Barbet-Massin, E.; Sormanni, P.; Barbiroli, A.; Porcari, R.; Mota, C. S.; et al. Conformational dynamics in crystals reveal the molecular bases for D76N beta-2 microglobulin aggregation propensity. *Nat. Commun.* **2018**, *9*, No. 1658.

(198) Smith, A. A.; Testori, E.; Cadalbert, R.; Meier, B. H.; Ernst, M. Characterization of fibril dynamics on three timescales by solid-state NMR. *J. Biomol. NMR* **2016**, *65*, 171−191.

(199) Fry, E. A.; Sengupta, S.; Phan, V. C.; Kuang, S.; Zilm, K. W. CSA-Enabled Spin Diffusion Leads to MAS Rate-Dependent T-1's at High Field. *J. Am. Chem. Soc.* **2011**, *133*, 1156−1158.

(200) Asami, S.; Porter, J. R.; Lange, O. F.; Reif, B. Access to Cα backbone dynamics of biological solids by (13)C-T1 relaxation and molecular dynamics simulation. *J. Am. Chem. Soc.* **2015**, *137*, 1094−1100.

(201) Smith, A. A.; Ernst, M.; Meier, B. H. Because the Light is Better Here: Correlation-Time Analysis by NMR Spectroscopy. *Angew. Chem., Int. Ed.* **2017**, *56*, 13590−13595.

(202) Lewandowski, J. R.; Sass, H. J.; Grzesiek, S.; Blackledge, M.; Emsley, L. Site-Specific Measurement of Slow Motions in Proteins. *J. Am. Chem. Soc.* **2011**, *133*, 16762−16765.

(203) Krushelnitsky, A.; Zinkevich, T.; Reif, B.; Saalwächter, K. Slow motions in microcrystalline proteins as observed by MAS-dependent 15N rotating-frame NMR relaxation. *J. Magn. Reson.* **2014**, *248*, 8−12.

(204) Rovo, P.; Linser, R. Microsecond Timescale Protein Dynamics: a Combined Solid-State NMR Approach. *ChemPhysChem* **2018**, *19*, 34−39.

(205) Lewandowski, J. R.; Sein, J.; Blackledge, M.; Emsley, L. Anisotropic Collective Motion Contributes to Nuclear Spin Relaxation in Crystalline Proteins. *J. Am. Chem. Soc.* **2010**, *132*, 1246−1248.

(206) Ma, P. X.; Xue, Y.; Coquelle, N.; Haller, J. D.; Yuwen, T. R.; Ayala, I.; Mikhailovskii, O.; Willbold, D.; Colletier, J. P.; Skrynnikov, N. R.; Schanda, P. Observing the overall rocking motion of a protein in a crystal. *Nat. Commun.* **2015**, *6*, No. 8361.

(207) Kurauskas, V.; Izmailov, S. A.; Rogacheva, O. N.; Hessel, A.; Ayala, I.; Woodhouse, J.; Shilova, A.; Xue, Y.; Yuwen, T. R.; Coquelle, N.; et al. Slow conformational exchange and overall rocking motion in ubiquitin protein crystals. *Nat. Commun.* **2017**, *8*, No. 145.

(208) Krushelnitsky, A.; Gauto, D.; Rodriguez Camargo, D. C.; Schanda, P.; Saalwachter, K. Microsecond motions probed by near-rotary-resonance R (1 rho) N-15 MAS NMR experiments: the model case of protein overall-rocking in crystals. *J. Biomol. NMR* **2018**, *71*, 53−67.

(209) Kurbanov, R.; Zinkevich, T.; Krushelnitsky, A. The nuclear magnetic resonance relaxation data analysis in solids: General R-1/R-1 rho equations and the model-free approach. *J. Chem. Phys.* **2011**, *135*, No. 184104.

(210) Marion, D.; Gauto, D. F.; Ayala, I.; Giandoreggio-Barranco, K.; Schanda, P. Microsecond Protein Dynamics from Combined Bloch-McConnell and Near-Rotary-Resonance R-1p Relaxation-Dispersion MAS NMR. *ChemPhysChem* **2019**, *20*, 276−284.

(211) Shannon, M. D.; Theint, T.; Mukhopadhyay, D.; Surewicz, K.; Surewicz, W. K.; Marion, D.; Schanda, P.; Jaroniec, C. P. Conforma-

https://doi.org/10.1021/acs.chemrev.1c00681
Chem. Rev. XXXX, XXX, XXX−XXX

tional Dynamics in the Core of Human Y145Stop Prion Protein Amyloid Probed by Relaxation Dispersion NMR. *ChemPhysChem* **2019**, *20*, 311−317.

(212) Gauto, D. F.; Hessel, A.; Rovo, P.; Kurauskas, V.; Linser, R.; Schanda, P. Protein conformational dynamics studied by N-15 and H-1 R-1rho relaxation dispersion: Application to wild-type and G53A ubiquitin crystals. *Solid State Nucl. Magn. Reson.* **2017**, *87*, 86−95.

(213) Rovo, P.; Smith, C. A.; Gauto, D.; de Groot, B. L.; Schanda, P.; Linser, R. Mechanistic Insights into Microsecond Time-Scale Motion of Solid Proteins Using Complementary N-15 and H-1 Relaxation Dispersion Techniques. *J. Am. Chem. Soc.* **2019**, *141*, 858−869.

(214) Takegoshi, K.; Terao, T. C-13 nuclear Overhauser polarization nuclear magnetic resonance in rotating solids: Replacement of cross polarization in uniformly C-13 labeled molecules with methyl groups. *J. Chem. Phys.* **2002**, *117*, 1700−1707.

(215) Katoh, E.; Takegoshi, K.; Terao, T. C-13 nuclear overhauser polarization-magic-angle spinning nuclear magnetic resonance spectroscopy in uniformly C-13-labeled solid proteins. *J. Am. Chem. Soc.* **2004**, *126*, 3653−3657.

(216) Purusottam, R. N.; Bodenhausen, G.; Tekely, P. Quantitative one- and two-dimensional C-13 spectra of microcrystalline proteins with enhanced intensity. *J. Biomol. NMR* **2013**, *57*, 11−19.

(217) Purusottam, R. N.; Tekely, P. Site-specific dynamics of methyl groups probed by temporal evolution of heteronuclear C-13{H-1} Overhauser polarisation encoded in C-13-C-13 solid-state NMR correlation experiments. *Chem. Phys. Lett.* **2020**, *754*, No. 137628.

(218) Giraud, N.; Sein, J.; Pintacuda, G.; Böckmann, A.; Lesage, A.; Blackledge, M.; Emsley, L. Observation of Heteronuclear Overhauser Effects Confirms the 15N-1H Dipolar Relaxation Mechanism in a Crystalline Protein. *J. Am. Chem. Soc.* **2006**, *128*, 12398−12399.

(219) Lopez del Amo, J. M.; Agarwal, V.; Sarkar, R.; Porter, J.; Asami, S.; Rubbelke, M.; Fink, U.; Xue, Y.; Lange, O. F.; Reif, B. Site-specific analysis of heteronuclear NOE effects in microcrystalline proteins. *J. Biomol. NMR* **2014**, *59*, 241−249.

(220) Mao, J. F.; Aladin, V.; Jin, X. S.; Leeder, A. J.; Brown, L. J.; Brown, R. C. D.; He, X.; Corzilius, B.; Glaubitz, C. Exploring Protein Structures by DNP-Enhanced Methyl Solid-State NMR Spectroscopy. *J. Am. Chem. Soc.* **2019**, *141*, 19888−19901.

(221) Chevelkov, V.; Xue, Y.; Linser, R.; Skrynnikov, N. R.; Reif, B. Comparison of Solid-State Dipolar Couplings and Solution Relaxation Data Provides Insight into Protein Backbone Dynamics. *J. Am. Chem. Soc.* **2010**, *132*, 5015−5017.

(222) Smith, A. A.; Ernst, M.; Riniker, S.; Meier, B. H. Localized and Collective Motions in HET-s(218−289) Fibrils from Combined NMR Relaxation and MD Simulation. *Angew. Chem., Int. Ed.* **2019**, *58*, 9383−9388.

(223) Grohe, K.; Patel, S.; Hebrank, C.; Medina, S.; Klein, A.; Rovo, P.; Vasa, S. K.; Singh, H.; Vogeli, B.; Schafer, L. V.; et al. Protein Motional Details Revealed by Complementary Structural Biology Techniques. *Structure* **2020**, *28*, 1024−1034.

(224) Lakomek, N. A.; Penzel, S.; Lends, A.; Cadalbert, R.; Ernst, M.; Meier, B. H. Microsecond Dynamics in Ubiquitin Probed by Solid-State N-15 NMR Spectroscopy R-1 rho Relaxation Experiments under Fast MAS (60−110 kHz). *Chem. - Eur. J.* **2017**, *23*, 9425−9433.

(225) Saurel, O.; Iordanov, I.; Nars, G.; Demange, P.; Le Marchand, T.; Andreas, L. B.; Pintacuda, G.; Milon, A. Local and Global Dynamics in Klebsiella pneumoniae Outer Membrane Protein a in Lipid Bilayers Probed at Atomic Resolution. *J. Am. Chem. Soc.* **2017**, *139*, 1590−1597.

(226) Schubeis, T.; Schwarzer, T. S.; Le Marchand, T.; Stanek, J.; Movellan, K. T.; Castiglione, K.; Pintacuda, G.; Andreas, L. B. Resonance assignment of the outer membrane protein AlkL in lipid bilayers by proton-detected solid-state NMR. *Biomol. NMR Assignments* **2020**, *14*, 295−300.

(227) Schubeis, T.; Le Marchand, T.; Daday, C.; Kopec, W.; Tekwani Movellan, K.; Stanek, J.; Schwarzer, T. S.; Castiglione, K.; de Groot, B. L.; Pintacuda, G.; Andreas, L. B. A beta-barrel for oil transport through lipid membranes: Dynamic NMR structures of AlkL. *Proc. Natl. Acad. Sci. U. S. A.* **2020**, *117*, 21014−21021.

(228) Bonaccorsi, M.; Knight, M. J.; Le Marchand, T.; Dannatt, H. R. W.; Schubeis, T.; Salmon, L.; Felli, I. C.; Emsley, L.; Pierattelli, R.; Pintacuda, G. Multimodal Response to Copper Binding in Superoxide Dismutase Dynamics. *J. Am. Chem. Soc.* **2020**, *142*, 19660−19667.

(229) Singh, H.; Vasa, S. K.; Jangra, H.; Rovo, P.; Paslack, C.; Das, C. K.; Zipse, H.; Schafer, L. V.; Linser, R. Fast Microsecond Dynamics of the Protein-Water Network in the Active Site of Human Carbonic Anhydrase II Studied by Solid-State NMR Spectroscopy. *J. Am. Chem. Soc.* **2019**, *141*, 19276−19288.

(230) Singh, H.; Das, C. K.; Vasa, S. K.; Grohe, K.; Schafer, L. V.; Linser, R. The Active Site of a Prototypical "Rigid" Drug Target is Marked by Extensive Conformational Dynamics. *Angew. Chem., Int. Ed.* **2020**, *59*, 22916−22921.

(231) Felix, J.; Weinhaupl, K.; Chipot, C.; Dehez, F.; Hessel, A.; Gauto, D. F.; Morlot, C.; Abian, O.; Gutsche, I.; Velazquez-Campoy, A.; Schanda, P.; Fraga, H. Mechanism of the allosteric activation of the ClpP protease machinery by substrates and active-site inhibitors. *Sci. Adv.* **2019**, *5*, No. aaw3818.

(232) Chevelkov, V.; Reif, B. TROSY effects in MAS solid-state NMR. *Concepts Magn. Reson., Part A* **2008**, *32A*, 143−156.

(233) Linser, R.; Fink, U.; Reif, B. Assignment of Dynamic Regions in Biological Solids Enabled by Spin-State Selective NMR Experiments. *J. Am. Chem. Soc.* **2010**, *132*, 8891−8893.

(234) Pervushin, K.; Riek, R.; Wider, G.; Wüthrich, K. Attenuated T2 relaxation by mutual cancellation of dipole-dipole coupling and chemical shift anisotropy indicates an avenue to NMR structures of very large biological macromolecules in solution. *Proc. Natl. Acad. Sci. U. S. A.* **1997**, *94*, 12366−12371.

(235) Linser, R.; Dasari, M.; Hiller, M.; Higman, V.; Fink, U.; Lopez del Amo, J.-M.; Handel, L.; Kessler, B.; Schmieder, P.; Oesterhelt, D.; et al. Proton detected solid-state NMR of fibrillar and membrane proteins. *Angew. Chem., Int. Ed.* **2011**, *50*, 4508−4512.

(236) Morris, V. K.; Linser, R.; Wilde, K. L.; Duff, A. P.; Sunde, M.; Kwan, A. H. Solid-State NMR Spectroscopy of Functional Amyloid from a Fungal Hydrophobin: A Well-Ordered beta-Sheet Core Amidst Structural Heterogeneity. *Angew. Chem., Int. Ed.* **2012**, *51*, 12621−12625.

(237) Mainz, A.; Jehle, S.; van Rossum, B. J.; Oschkinat, H.; Reif, B. Large Protein Complexes with Extreme Rotational Correlation Times Investigated in Solution by Magic-Angle-Spinning NMR Spectroscopy. *J. Am. Chem. Soc.* **2009**, *131*, 15968−15969.

(238) Bertini, I.; Luchinat, C.; Parigi, G.; Ravera, E.; Reif, B.; Turano, P. Solid-state NMR of proteins sedimented by ultracentrifugation. *Proc. Natl. Acad. Sci. U. S. A.* **2011**, *108*, 10396−10399.

(239) Bertini, I.; Luchinat, C.; Parigi, G.; Ravera, E. SedNMR: On the Edge between Solution and Solid-State NMR. *Acc. Chem. Res.* **2013**, *46*, 2059−2069.

(240) Böckmann, A.; Gardiennet, C.; Verel, R.; Hunkeler, A.; Loquet, A.; Pintacuda, G.; Emsley, L.; Meier, B. H.; Lesage, A. Characterization of different water pools in solid-state NMR protein samples. *J. Biomol. NMR* **2009**, *45*, 319−327.

(241) Bertini, I.; Engelke, F.; Gonnelli, L.; Knott, B.; Luchinat, C.; Osen, D.; Ravera, E. On the use of ultracentrifugal devices for sedimented solute NMR. *J. Biomol. NMR* **2012**, *54*, 123−127.

(242) Gardiennet, C.; Schutz, A. K.; Hunkeler, A.; Kunert, B.; Terradot, L.; Böckmann, A.; Meier, B. H. A Sedimented Sample of a 59 kDa Dodecameric Helicase Yields High-Resolution Solid-State NMR Spectra. *Angew. Chem., Int. Ed.* **2012**, *51*, 7855−7858.

(243) Hisao, G. S.; Harland, M. A.; Brown, R. A.; Berthold, D. A.; Wilson, T. E.; Rienstra, C. M. An efficient method and device for transfer of semisolid materials into solid-state NMR spectroscopy rotors. *J. Magn. Reson.* **2016**, *265*, 172−176.

(244) Mandal, A.; Boatz, J. C.; Wheeler, T. B.; van der Wel, P. C. A. On the use of ultracentrifugal devices for routine sample preparation in biomolecular magic-angle-spinning NMR. *J. Biomol. NMR* **2017**, *67*, 165−178.

(245) Stevens, R. A. The Development of Solid-State NMR Methodology to Study the Dynamics of Proteins and Ice. Ph.D. thesis. Chemistry Department, University of Warwick, UK, 2018.

https://doi.org/10.1021/acs.chemrev.1c00681
Chem. Rev. XXXX, XXX, XXX−XXX

(246) Mainz, A.; Religa, T.; Sprangers, R.; Linser, R.; Kay, L. E.; Reif, B. NMR Spectroscopy of Soluble Protein Complexes at One Mega-Dalton and Beyond. *Angew. Chem., Int. Ed.* **2013**, *52*, 8746−8751.
(247) Kurauskas, V.; Crublet, E.; Macek, P.; Kerfah, R.; Gauto, D. F.; Boisbouvier, J.; Schanda, P. Sensitive proton-detected solid-state NMR spectroscopy of large proteins with selective CH3 labelling: application to the 50S ribosome subunit. *Chem. Commun.* **2016**, *52*, 9558−9561.
(248) Barbet-Massin, E.; van der Sluis, E.; Musial, J.; Beckmann, R.; Reif, B. Reconstitution of Isotopically Labeled Ribosomal Protein L29 in the 50S Large Ribosomal Subunit for Solution-State and Solid-State NMR. *Methods Mol. Biol.* **2018**, *1764*, 87−100.
(249) Barbet-Massin, E.; Huang, C.-T.; Daebel, V.; Hsu, S.-T. D.; Reif, B. Site-Specific Solid-State NMR Studies of "Trigger Factor" in Complex with the Large Ribosomal Subunit 50S. *Angew. Chem., Int. Ed.* **2015**, *54*, 4367−4369.
(250) Mainz, A.; Peschek, J.; Stavropoulou, M.; Back, K.; Bardiaux, B.; Asami, S.; Prade, E.; Peters, C.; Weinkauf, S.; Buchner, J.; et al. The Chaperone αB-Crystallin Deploys Different Interfaces to Capture an Amorphous and an Amyloid Client. *Nat. Struct. Mol. Biol.* **2015**, *22*, 898−905.
(251) Jehle, S.; van Rossum, B.-J.; Stout, J. R.; Noguchi, S. M.; Falber, K.; Rehbein, K.; Oschkinat, H.; Klevit, R. E.; Rajagopal, P. alpha B-Crystallin: A Hybrid Solid-State/Solution-State NMR Investigation Reveals Structural Aspects of the Heterogeneous Oligomer. *J. Mol. Biol.* **2009**, *385*, 1481−1497.
(252) Dannatt, H. R. W.; Felletti, M.; Jehle, S.; Wang, Y.; Emsley, L.; Dixon, N. E.; Lesage, A.; Pintacuda, G. Weak and Transient Protein Interactions Determined by Solid-State NMR. *Angew. Chem., Int. Ed.* **2016**, *55*, 6638−6640.
(253) Damman, R.; Schutz, S.; Luo, Y. Z.; Weingarth, M.; Sprangers, R.; Baldus, M. Atomic-level insight into mRNA processing bodies by combining solid and solution-state NMR spectroscopy. *Nat. Commun.* **2019**, *10*, No. 4536.
(254) Maybury, R. H.; Katz, J. J. Protein denaturation in heavy water. *Nature* **1956**, *177*, 629−630.
(255) Makhatadze, G. I.; Clore, G. M.; Gronenborn, A. M. Solvent Isotope Effect and Protein Stability. *Nat. Struct. Biol.* **1995**, *2*, 852−855.
(256) Stadmiller, S. S.; Pielak, G. J. Enthalpic stabilization of an SH3 domain by D2O. *Protein Sci.* **2018**, *27*, 1710−1716.
(257) Turowski, M.; Yamakawa, N.; Meller, J.; Kimata, K.; Ikegami, T.; Hosoya, K.; Tanaka, N.; Thornton, E. R. Deuterium isotope effects on hydrophobic interactions: The importance of dispersion interactions in the hydrophobic phase. *J. Am. Chem. Soc.* **2003**, *125*, 13836−13849.
(258) Nichols, P. J.; Falconer, I.; Griffin, A.; Mant, C.; Hodges, R.; McKnight, C. J.; Vogeli, B.; Vugmeyster, L. Deuteration of nonexchangeable protons on proteins affects their thermal stability, side-chain dynamics, and hydrophobicity. *Protein Sci.* **2020**, *29*, 1641−1654.
(259) Yee, A. W.; Moulin, M.; Breteau, N.; Haertlein, M.; Mitchell, E. P.; Cooper, J. B.; Boeri Erba, E.; Forsyth, V. T. Impact of Deuteration on the Assembly Kinetics of Transthyretin Monitored by Native Mass Spectrometry and Implications for Amyloidoses. *Angew. Chem., Int. Ed.* **2016**, *55*, 9292−9296.
(260) Brockwell, D.; Yu, L.; Cooper, S.; McCleland, S.; Cooper, A.; Attwood, D.; Gaskell, S. J.; Barber, J. Physicochemical consequences of the perdeuteriation of glutathione S-transferase from S. japonicum. *Protein Sci.* **2001**, *10*, 572−580.
(261) Meilleur, F.; Contzen, J.; Myles, D. A. A.; Jung, C. Structural stability and dynamics of hydrogenated and perdeuterated cytochrome P450cam (CYP101). *Biochemistry* **2004**, *43*, 8744−8753.
(262) Piszczek, G.; Lee, J. C.; Tjandra, N.; Lee, C. R.; Seok, Y. J.; Levine, R. L.; Peterkofsky, A. Deuteration of Escherichia coli Enzyme I-Ntr alters its stability. *Arch. Biochem. Biophys.* **2011**, *507*, 332−342.
(263) Schubeis, T.; Le Marchand, T.; Andreas, L. B.; Pintacuda, G. H-1 magic-angle spinning NMR evolves as a powerful new tool for membrane proteins. *J. Magn. Reson.* **2018**, *287*, 140−152.
(264) Chen, P. H.; Albert, B. J.; Gao, C. K.; Alaniva, N.; Price, L. E.; Scott, F. J.; Saliba, E. P.; Sesti, E. L.; Judge, P. T.; Fisher, E. W.; et al. Magic angle spinning spheres. *Sci. Adv.* **2018**, *4*, No. aau1540.
(265) Gao, C. K.; Judge, P. T.; Sesti, E. L.; Price, L. E.; Alaniva, N.; Saliba, E. P.; Albert, B. J.; Soper, N. J.; Chen, P. H.; Barnes, A. B. Four millimeter spherical rotors spinning at 28 kHz with double-saddle coils for cross polarization NMR. *J. Magn. Reson.* **2019**, *303*, 1−6.
(266) Penzel, S.; Oss, A.; Org, M. L.; Samoson, A.; Böckmann, A.; Ernst, M.; Meier, B. H. Spinning faster: protein NMR at MAS frequencies up to 126kHz. *J. Biomol. NMR* **2019**, *73*, 19−29.
(267) Schledorn, M.; Malar, A. A.; Torosyan, A.; Penzel, S.; Klose, D.; Oss, A.; Org, M. L.; Wang, S. S.; Lecoq, L.; Cadalbert, R.; et al. Protein NMR Spectroscopy at 150 kHz Magic-Angle Spinning Continues To Improve Resolution and Mass Sensitivity. *ChemBioChem* **2020**, *21*, 2540−2548.
(268) Iwasa, Y.; Bascunan, J.; Hahn, S.; Voccio, J.; Kim, Y.; Lecrevisse, T.; Song, J.; Kajikawa, K. A High-Resolution 1.3-GHz/54-mm LTS/HTS NMR Magnet. *IEEE Trans. Appl. Supercond.* **2015**, *25*, No. 4301205.
(269) Gan, Z. H.; Hung, I.; Wang, X. L.; Paulino, J.; Wu, G.; Litvak, I. M.; Gor'kov, P. L.; Brey, W. W.; Lendi, P.; Schiano, J. L.; et al. NMR spectroscopy up to 35.2 T using a series-connected hybrid magnet. *J. Magn. Reson.* **2017**, *284*, 125−136.
(270) Hoult, D. I.; Richards, R. E. Signal-to-noise ratio of a nuclear magnetic-resonance experiment. *J. Magn. Reson.* **1976**, *24*, 71−85.
(271) Xue, K.; Sarkar, R.; Lalli, D.; Koch, B.; Pintacuda, G.; Tošner, Z.; Reif, B. Impact of magnetic field strength on resolution and sensitivity of proton resonances in biological solids. *J. Phys. Chem. C* **2020**, *124*, 22631−22637.
(272) Nimerovsky, E.; Movellan, K. T.; Zhang, X. C.; Forster, M. C.; Najbauer, E.; Xue, K.; Dervisoglu, R.; Giller, K.; Griesinger, C.; Becker, S.; et al. Proton Detected Solid-State NMR of Membrane Proteins at 28 T (1.2 GHz) and 100 kHz Magic-Angle Spinning. *Biomolecules* **2021**, *11*, No. 752.
(273) Callon, M.; Malär, A. A.; Pfister, S.; Římal, V.; Weber, M. E.; Wiegand, T.; Zehnder, J.; Chávez, M.; Cadalbert, R.; Deb, R.; et al. Biomolecular solid-state NMR spectroscopy at 1200 MHz: the gain in resolution. *J. Biomol. NMR* **2021**, *75*, 255−272.
(274) Xue, K.; Sarkar, R.; Motz, C.; Asami, S.; Rodriguez Camargo, D. C.; Decker, V.; Wegner, S.; Tošner, Z.; Reif, B. Limits of Resolution and Sensitivity of Proton Detected MAS Solid-State NMR Experiments at 111 kHz in Deuterated and Protonated Proteins. *Sci. Rep.* **2017**, *7*, No. 7444.

https://doi.org/10.1021/acs.chemrev.1c00681
Chem. Rev. XXXX, XXX, XXX−XXX